UC Santa Cruz
UC Santa Cruz Electronic Theses and Dissertations

Title
On the Dynamics of Inverse Magnetic Billiards

Permalink
https://escholarship.org/uc/item/4dn4d2z1

Author
Gasiorek, Sean

Publication Date
2019

Copyright Information

Peer reviewed|Thesis/dissertation

UNIVERSITY OF CALIFORNIA

SANTA CRUZ

ON THE DYNAMICS OF INVERSE MAGNETIC BILLIARDS

A dissertation submitted in partial satisfaction of the
requirements for the degree of

DOCTOR OF PHILOSOPHY

in

MATHEMATICS

by

Sean Gasiorek

June 2019

The Dissertation of Sean Gasiorek
is approved:

_____

Professor Richard Montgomery, Chair

_____

Professor Debra Lewis

_____

Professor Jie Qing

_____

Lori Kletzer
Vice Provost and Dean of Graduate Studies

Table of Contents

List of Figures

Abstract

On the Dynamics of Inverse Magnetic Billiards

by

Sean Gasiorek

Consider a strictly convex set Ω in the plane, and a homogeneous, stationary magnetic field orthogonal to the plane whose strength is B on the complement of Ω and 0 inside Ω. The trajectories of a charged particle in this setting are straight lines concatenated with circular arcs of Larmor radius μ. We examine the dynamics of such a particle and call this *inverse magnetic billiards*. Comparisons are made to standard Birkhoff billiards and magnetic billiards, as some theorems regarding inverse magnetic billiards are consistent with each of these billiard variants while others are not.

Acknowledgments

 I first and foremost wish to thank my wife Danielle for her love and support throughout my many years pursuing this goal. It cannot be easy being married to a graduate student, much less a mathematician and all that entails.

I am thankful for my advisor, Richard Montgomery, for his insight, knowledge, and patience throughout our multiple mathematical endeavors, and for guiding me into the world of mathematics research. I am grateful for Professors Sergei Tabachnikov and Alfonso Sorrentino for their helpful billiards discussions during our time at MSRI in Fall, 2018.

I would like to thank my mathematical siblings Gabe, Connor, Andres, and Steven for always being willing to talk about our work and learn from each other over the years. I also am thankful for my fellow graduate students throughout my six years in Santa Cruz, of which there are too many to name, for their friendship inside and outside the classroom.

I also wish to thank my mathematical family from my eight years in San Luis Obispo. As a student, Katie, Wade, Kendall, Erin, Jeremy, Suz, Richard, and Mike helped shape me into the budding mathematician I am today. As a teacher, Dylan, Vince, Bill, Jeff, Morgan, Rob, Dana, Todd, and many more have helped me become the mathematics educator that I always admired in them and continue to aspire to become in my years ahead in academia.

I want to thank the many inspiring math teachers I have had over the years. Their passion for mathematics and teaching has put me on this trajectory, and I hope to continue to honor what they have instilled in me throughout the rest of my personal and professional life.

And lastly, I want to thank my parents and family for their support, without which this would not have been possible. This includes, but is not limited to,

Chapter 1

Introduction

1.1 Preliminaries

We consider the classical motion of a particle of mass m and charge e in the plane. Let $\Omega \subset \mathbb{R}^2$ denote a connected, strictly convex domain, and define a constant, homogeneous, stationary magnetic field orthogonal to the plane which has strength B on $\mathbb{R}^2 \setminus \Omega$ and 0 on Ω. As such, the equations of motion for the particle of position q and velocity v are as follows:

$$\begin{cases} \dot{q} & = v \\ \dot{v} & = B_\Omega(q)\mathbb{J}v \end{cases} \quad \text{with} \quad \mathbb{J} := \begin{pmatrix} 0 & -1 \\ 1 & 0 \end{pmatrix}, \quad B_\Omega(q) := \begin{cases} 0 & q \in \Omega \\ B & q \in \mathbb{R}^2 \setminus \Omega \end{cases}.$$

The solution to this initial value problem will produce circular arcs outside of Ω and straight lines inside Ω. The circular arcs will have Larmor radius $\mu = \frac{m|v|}{|eB|}$, and speed $|\dot{q}|$ and energy E are constants of motion. Without loss of generality we assume $e < 0$ and $B > 0$ so that the motion along the circular arcs of radius μ will be traversed in the counterclockwise direction.

In general we will want $\partial\Omega$ to consist of simple, closed, C^k curves of total length

1

$|\partial\Omega| = L$. Occasionally we may relax some of these conditions, but this will be indicated when necessary. The boundary $\partial\Omega = Image(\Gamma(s))$ will be parametrized by arc length, s:

$$\Gamma(s) = (X(s), Y(s)), \quad ds^2 = dX^2 + dY^2, \quad s \in \mathbb{R}/L\mathbb{Z}.$$

The unit tangent and unit normal vectors and the signed curvature are given by

$$\boldsymbol{t}(s) = (X'(s), Y'(s)) = (\cos(\tau(s)), \sin(\tau(s))),$$

$$\boldsymbol{n}(s) = (-Y'(s), X'(s)),$$

$$\kappa(s) = \frac{d\tau}{ds} = X'(s)Y''(s) - X''(s)Y'(s) = \frac{1}{\rho(s)},$$

so that $\tau(s)$ is the polar angle between the positive x-axis and $\boldsymbol{t}(s)$, and $\rho(s)$ is the radius of curvature. Assume Ω is strictly convex so that the curvature of the boundary is strictly positive. Then $\rho(s)$ is bounded by positive constants, $0 < \rho_{min} \leq \rho(s) \leq \rho_{max} < \infty$ for all s. Following the lead of [RB85], we will explore the dynamics of our system in terms of the relative sizes of the Larmor radius μ and the maximum and minimum radii of curvature of $\partial\Omega$. We will refer to these possibilities

$$\mu < \rho_{min}, \qquad \rho_{min} < \mu < \rho_{max}, \qquad \rho_{max} < \mu$$

as *curvature regimes*.

The billiard flow is hence given by the Lagrangian

$$\mathcal{L}(q, \dot{q}) = \frac{1}{2}m|\dot{q}|^2 + e\langle \dot{q}, \mathbb{A}(q)\rangle, \quad \mathbb{A}(q) = \frac{1}{2}(-yB_\Omega(q), xB_\Omega(q)) = \frac{1}{2}B_\Omega(q)\mathbb{J}q$$

where $\langle \cdot, \cdot \rangle$ is the standard Euclidean inner product. We call this dynamical system

inverse magnetic billiards, following the naming by [VTCP03].

1.2 Previous Results

Standard "Birkhoff" billiards is a vast, well-studied subject with many open questions which began over a century ago (see books [TS05], [KT91], [CM06], for example). Magnetic billiards, where a homogeneous magnetic filed is placed inside the billiard table and the billiard ball is seen as a charged particle, was first studied by Robnik and Berry in the 1980's ([Rob86], [RB85]) and rigorously studied by Berglund and Kunz in the 1990's ([BK96], [Ber96]). In fact, outer magnetic billiards is briefly discussed in [BK96] but only in the context of boundaries with negative curvature and the duality of inner and outer magnetic billiards. However, inverse magnetic billiards has not been studied thoroughly.

In [KS17], a "magnetic bump" or "quantum dot" is studied where there is a magnetic field inside some convex set and no magnetic field outside the set. A charged particle is then scattered by encountering such a magnetic bump, and the symbolic dynamics of a sequence of such dots shows hyperbolic behavior. Further, in [KSS13], if the magnetic bumps are assumed to have a rotationally symmetric magnetic field inside, this dynamical system with ≥ 2 bumps exhibits chaotic behavior and positive topological entropy.

Systems of magnetic bumps and electron dynamics in piecewise-constant magnetic fields are further studied in [SG10], [Nog10], [SIKL98], [KPC05], [CP12], and [KROC08]. Classical, semiclassical, and quantum approaches to this system are each addressed to a degree – occasionally in compact subsets and sometimes in unbounded regions – but none are in-depth mathematically to the extent of, say, [BK96] with respect to magnetic billiards.

The system of inverse magnetic billiards has been briefly studied in the context

of condensed-matter physics. Developments in nanotechnology have allowed for confinement of charged particles modeled by a 2-dimensional electron gas (2DEG) in an inhomogeneous magnetic field, and for certain nanostructures the electron's dynamics are dominated by classical kinematic motion with no concern or influence of quantum effects. The inhomogeneous or piecewise-constant magnetic field can be realized by placing a superconductor over the 2DEG, or by changing physical characteristics of the environment of the 2DEG. In [VTCP03], the dynamics of inverse magnetic billiards is studied numerically in a piecewise-constant magnetic field to find two quantities for the Bunimovich stadium (a rectangle with two of its opposing sides capped by semicircles): the Lyapunov exponent and the integrable/chaotic phase space ratio, each as a function of the magnetic field strength B. Their findings indicate both quantities are smooth functions of B, and there is a smooth transition from chaos ($B = \infty$), a known billiard result, to integrable ($B = 0$). From this they conclude that the level of chaos in inverse magnetic billiards in the Bunimovich stadium is controllable.

Chapter 2

Properties of the Inverse Magnetic Billiard Map

2.1 Constructing the Return Map and its Jacobian

As the particle moves, it successively leaves and re-enters Ω at points $P_0, P_1,$ $P_2, \ldots \in \partial\Omega$. Index these points so that points with even index $P_0, P_2, P_4, \ldots$ are re-entry points and points $P_1, P_3, P_5, \ldots$ of odd index are exit points. Express the oriented line segment $P_0 P_1$ joining each entry point to its successive exit point as a vector $\ell_1 \vec{v}_0 = P_1 - P_0$ where $\vec{v}_0$ is the unit vector representing the direction of motion of the particle while it travels inside Ω from P_0 to P_1 and where $\ell_1 = |P_1 - P_0|$ is the chord distance it travels.

The entire dynamics is summarized by the map $(P_0, v_0) \mapsto (P_2, v_2)$ taking reentry point and direction to successive re-entry point and direction. We call this map the *return map* and will express it in terms of the Birkhoff coordinates used in standard billiards. Coordinatize P_0 by its arc length parameter s_0 and the

vector v_0 by the negative cosine of the angle θ_0 between the tangent to Γ at P_0 and this vector. Writing $u_i = -\cos(\theta_i)$ we call (s_i, u_i) the Birkhoff coordinates of the trajectory as it re-enters Ω at P_i. Defining $\mathcal{P} = \mathbb{R}/L\mathbb{Z} \times [-1, 1] \cong S^1 \times [-1, 1]$, the return map T can then be written as a map

$$T : \mathcal{P} \to \mathcal{P}, \quad (s_0, u_0) \mapsto (s_2, u_2)$$

so that T is a smooth map of the closed annulus, $\mathcal{P}$. Further, the restriction $T|_{\partial\mathcal{P}} = \mathrm{Id}_{\mathcal{P}}$, where the boundary $\partial\mathcal{P}$ of $\mathcal{P}$ is the usual boundary of $\mathcal{P}$, namely $(S^1 \times \{-1\}) \cup (S^1 \times \{1\})$.

At times it may be easier to work with T as a map in terms of (s_i, θ_i) instead, and we will indicate as such when appropriate. In particular, we will compute Taylor expansions of T in Chapter 3 in terms of s and θ. With this interpretation, we see the inverse magnetic billiard as a discrete dynamical system.

Let $\ell_2 = |P_1 P_2|$. Define $\mathcal{A}$ to be the area between chord $P_1 P_2$ and $\Gamma(s)$, and let $\mathcal{S}$ be the area within the circular arc γ and outside Ω. Define χ to be the angle measured counterclockwise from $\overrightarrow{P_0 P_1}$ to $\overrightarrow{P_1 P_2}$. See Figure 2.1.

By construction, we see that the following restrictions hold:

$$0 < \theta_i < \pi \text{ for each } i$$

$$0 < \chi < \pi$$

$$0 < \ell_1 < Diam(\Omega)$$

$$0 < \ell_2 < \min\{2\mu, Diam(\Omega)\}$$

where $Diam(\Omega) = \max\limits_{a,b \in \Omega} d(a, b)$ is the diameter of Ω.

Furthermore, consider the magnetic arc, γ. Let the angle of such an arc be ψ, $\varepsilon = 2\pi - \psi$, δ is the angle between the chord $P_1 P_2$ and the radius of the arc

6
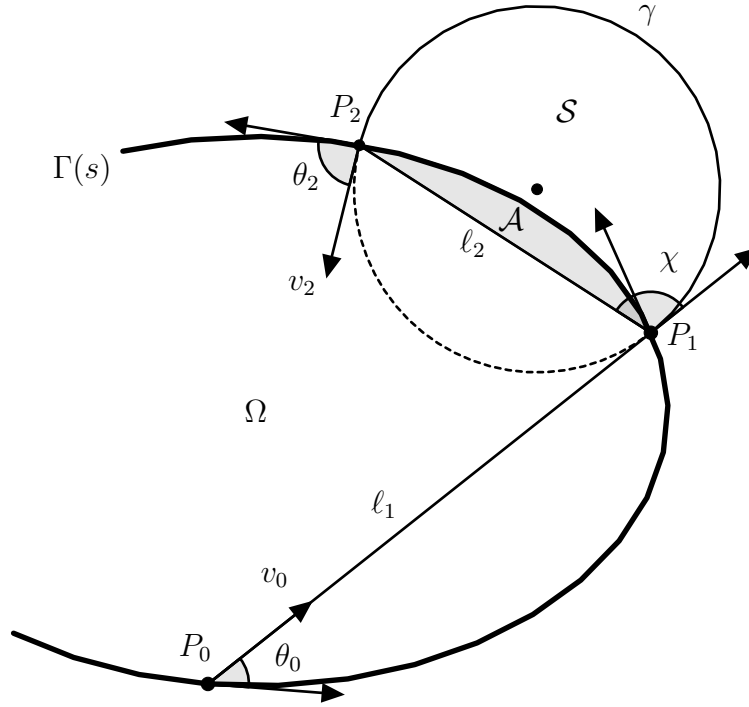
Figure 2.1: The standard picture of the return map, T.

connecting each of P_1 and P_2 to the center of γ. See Figure 2.2a.

From the definition of these angles we find the following to be true:

$$2\delta + \varepsilon = \pi$$

$$\psi + \varepsilon = 2\pi$$

$$\chi - \delta = \frac{\pi}{2}.$$

Solving this system and using elementary geometry yields

$$\psi = 2\chi \quad \text{and} \quad \sin(\chi) = \frac{\ell_2}{2\mu}.$$

It is important to note that there may be two trajectories with supplementary χ for a given chord length ℓ_2. See Figure 2.2b for such an example.
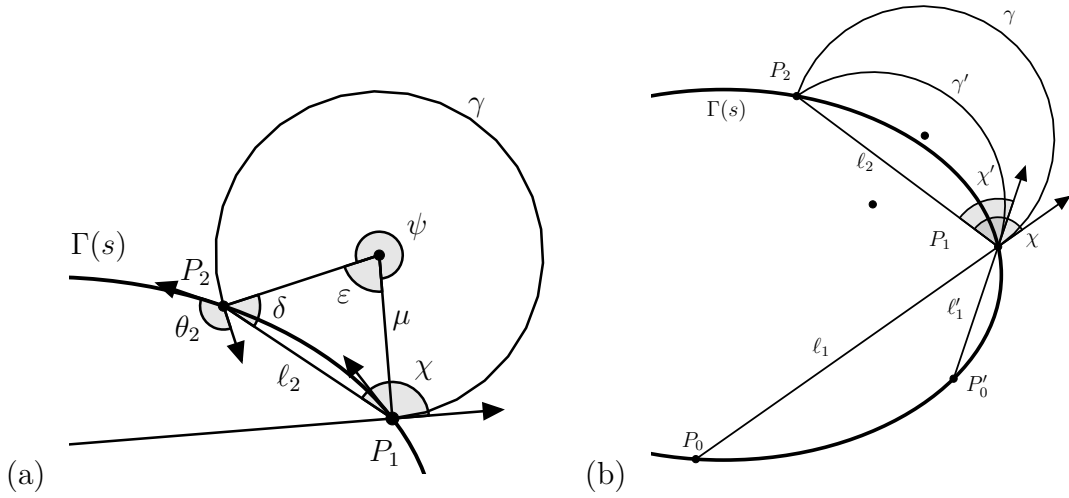
Figure 2.2: (a) A magnetic arc. (b) An example of two trajectories with the same value for ℓ_2 where χ and χ' are supplementary.

Proposition 1. *For small $\theta_1 > 0$, we can approximate χ as follows:*

$$\chi(\theta_1) \approx \begin{cases} \theta_1 + \arcsin\left(\frac{\mu \sin(\theta_1)}{\rho_1 - \mu}\right) & \text{if } \mu < \rho_{min} \\ \theta_1 + \pi - \arcsin\left(\frac{\mu \sin(\theta_1)}{-(\rho_1 - \mu)}\right) & \text{if } \rho_{max} < \mu. \end{cases}$$

and for $\theta_1 = \pi - \eta_1$ with small $\eta_1 > 0$,

$$\chi(\eta_1) \approx \pi - \eta_1 + \arcsin\left(\frac{\mu \sin(\eta_1)}{\rho_1 + \mu}\right).$$

See Appendix A.1 for the proof and for Taylor expansions of these expressions. These formulas will prove useful in due time.

We decompose T into its two distinct pieces. Define the map $T_1 : (s_0, u_0) \mapsto (s_1, u_1)$ as the analogue to the standard billiard map. The map $T_2 : (s_1, u_1) \mapsto (s_2, u_2)$ is the particle moving from P_1 along the circular arc γ of Larmor radius μ until intersecting $\partial\Omega$ again at P_2. Thus $T = T_2 \circ T_1$.
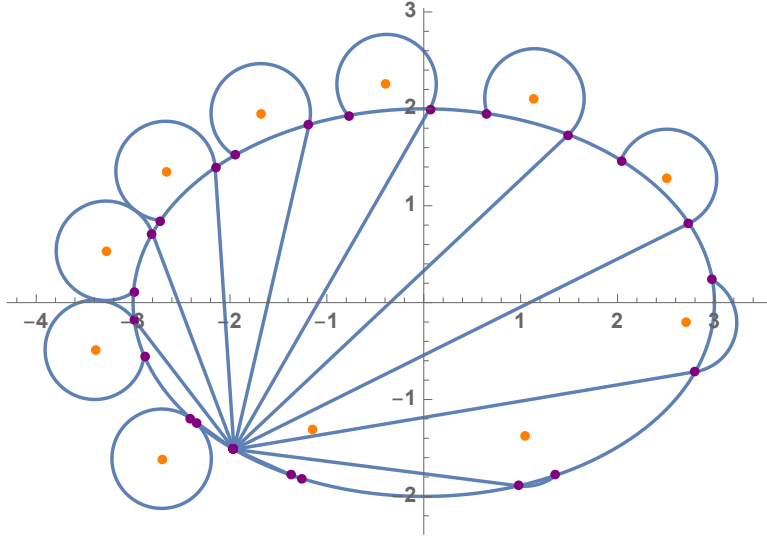
Figure 2.3: The behavior of the return map for fixed s_0 and varying u_0 when $\mu < \rho_{min}$. The Larmor centers are in orange and the dark purple points are P_0 and the corresponding P_1, P_2 for each value of u_0.

Proposition 2. *Given the maps T_1 and T_2, the Jacobians* $DT_1 = \begin{pmatrix} \frac{\partial s_1}{\partial s_0} & \frac{\partial s_1}{\partial u_0} \\ \frac{\partial u_1}{\partial s_0} & \frac{\partial u_1}{\partial u_0} \end{pmatrix}$

and $DT_2 = \begin{pmatrix} \frac{\partial s_2}{\partial s_1} & \frac{\partial s_2}{\partial u_1} \\ \frac{\partial u_2}{\partial s_1} & \frac{\partial u_2}{\partial u_1} \end{pmatrix}$ have components

$$\frac{\partial s_1}{\partial s_0} = \frac{\kappa_0 \ell_1 - \sin(\theta_0)}{\sin(\theta_1)}$$

$$\frac{\partial s_1}{\partial u_0} = \frac{\ell_1}{\sin(\theta_0)\sin(\theta_1)}$$

$$\frac{\partial u_1}{\partial s_0} = \kappa_0 \kappa_1 \ell_1 - \kappa_1 \sin(\theta_0) - \kappa_0 \sin(\theta_1)$$

$$\frac{\partial u_1}{\partial u_0} = \frac{\kappa_1 \ell_1 - \sin(\theta_1)}{\sin(\theta_0)}$$

$$\frac{\partial s_2}{\partial s_1} = \frac{\sin(2\chi - \theta_1) - \kappa_1 \ell_2 \cos(\chi)}{\sin(\theta_2)}$$

$$\frac{\partial s_2}{\partial u_1} = \frac{\ell_2 \cos(\chi)}{\sin(\theta_1)\sin(\theta_2)}$$

9

$$\frac{\partial u_2}{\partial s_1} = \frac{\sin(2\chi - \theta_1)\sin(2\chi - \theta_2) - \sin(\theta_1)\sin(\theta_2)}{\ell_2\cos(\chi)}$$

$$- \kappa_1\sin(2\chi - \theta_2) - \kappa_2\sin(2\chi - \theta_1) + \kappa_1\kappa_2\ell_2\cos(\chi)$$

$$\frac{\partial u_2}{\partial u_1} = \frac{\sin(2\chi - \theta_2) - \kappa_2\ell_2\cos(\chi)}{\sin(\theta_1)}.$$

Furthermore, $\det(DT_1) = 1$ *and* $\det(DT_2) = 1$.

The details of this proof are given in Appendix A.2. The components of DT_1 are well-known while the components of DT_2 are analogous to those found in Proposition 1 of [BK96].

Corollary 1. *Let* $T = T_2 \circ T_1$. *Then* $DT = \begin{pmatrix} \frac{\partial s_2}{\partial s_0} & \frac{\partial s_2}{\partial u_0} \\ \frac{\partial u_2}{\partial s_0} & \frac{\partial u_2}{\partial u_0} \end{pmatrix}$ *with*

$$\frac{\partial s_2}{\partial s_0} = \frac{\kappa_0\ell_1\sin(2\chi - \theta_1) - \sin(\theta_0)\sin(2\chi - \theta_1) - \kappa_0\ell_2\cos(\chi)\sin(\theta_1)}{\sin(\theta_1)\sin(\theta_2)}$$

$$\frac{\partial s_2}{\partial u_0} = \frac{\ell_1\sin(2\chi - \theta_1) - \ell_2\cos(\chi)\sin(\theta_1)}{\sin(\theta_0)\sin(\theta_1)\sin(\theta_2)}$$

$$\frac{\partial u_2}{\partial s_0} = \frac{\kappa_2\sin(\theta_0)\sin(2\chi - \theta_1)}{\sin(\theta_1)} + \frac{2\sin(\chi)\sin(2\chi - \theta_1 - \theta_2)(\kappa_0\ell_1 - \sin(\theta_0))}{\ell_2\sin(\theta_1)}$$

$$- \kappa_0\left(\sin(2\chi - \theta_2) + \frac{\kappa_2\ell_1\sin(2\chi - \theta_1)}{\sin(\theta_1)} - \kappa_2\ell_2\cos(\chi)\right)$$

$$\frac{\partial u_2}{\partial u_0} = \frac{\kappa_2\ell_2\cos(\chi) - \sin(2\chi - \theta_2)}{\sin(\theta_0)} + \frac{2\ell_1\sin(\chi)\sin(2\chi - \theta_1 - \theta_2) - \kappa_2\ell_1\ell_2\sin(2\chi - \theta_1)}{\ell_2\sin(\theta_0)\sin(\theta_1)}.$$

Furthermore, $\det(DT) = 1$.

From this we conclude that T is an area- and orientation-preserving map of the annulus $\mathcal{P}$ and that the Birkhoff coordinates are conjugate. Just as with standard billiards, the map T preserves the symplectic area-form $ds \wedge du = \sin(\theta)ds \wedge d\theta$ on $\mathcal{P}$.

2.2 Generating Functions and Twist Maps

We start with a tool that can be useful in the search for periodic orbits and for later use with variational methods.

Definition 1 ([Mei92]). *Let $T : (x, y) \mapsto (x', y')$ be a symplectic map from the annulus to itself, and suppose T is differentiable. Then T is a **twist map** (with a twist to the right) if there is a K such that*

$$\left.\frac{\partial x'}{\partial y}\right|_x \geq K > 0, \tag{2.2.1}$$

*so that x' is a monotonically increasing function of y. An analogous definition holds with reversed inequalities when defining a twist to the left. We call (2.2.1) the **twist condition**.*

Twist maps have many useful properties (see [Gol01], [Mei92]) relating to dynamics and symplectic geometry. For our purposes we take interest in the term

$$\frac{\partial s_2}{\partial u_0} = \frac{\ell_1 \sin(2\chi - \theta_1) - \ell_2 \cos(\chi) \sin(\theta_1)}{\sin(\theta_0) \sin(\theta_1) \sin(\theta_2)}.$$

Since $0 < \theta_i < \pi$, we see the denominator is always positive, but the numerator is of interest.

Proposition 3. *Let $\Gamma(s) = \partial\Omega$ be of class C^3 and let $\rho_{min} = \min\limits_{s \in [0, L)} \rho(s)$ be the minimum radius of curvature of the strictly convex boundary curve $\Gamma(s)$. Then if*

$$\mu < \rho_{min}$$

then

$$\ell_1 \sin(2\chi - \theta_1) - \ell_2 \cos(\chi) \sin(\theta_1) > 0.$$

We provide the details of this proof in Appendix A.3. But as an important corollary, we state the following:

Corollary 2. *If $\mu < \rho_{min}$, then the return map T is a twist map.*

An important distinction about this characterization is that when $\mu < \rho_{min}$, T is a twist map *for all* initial conditions (s_0, u_0). It is certainly possible that for some value of $\mu > \rho_{min}$ that $\ell_1 \sin(2\chi - \theta_1) - \ell_2 \cos(\chi) \sin(\theta_1) > 0$ for all iterations of T starting at a particular initial condition. Numerical experiments show that when u_0 is sufficiently close to 1, this twist condition is also satisfied, but this is not as strong as the statement above.

Next, we turn to another useful tool in understanding the dynamics of our system.

Definition 2. *A continuous map $T : \mathcal{P} \to \mathcal{P}$, $(s_0, u_0) \mapsto (s_2, u_2)$ has a real-valued function $G : S^1 \times S^1 \to \mathbb{R}$ as a **generating function** if $G(s_0, s_2)$ is a C^1 function such that*

$$dG = u_2 ds_2 - u_0 ds_0.$$

Alternately we may say $\frac{\partial G}{\partial s_0} = -u_0$ and $\frac{\partial G}{\partial s_2} = u_2$.

This generating function need not be unique. But in general we can think of the generating function as the reduced action along a solution ν to the Euler Lagrange equations which connects P_0 to P_2. See [BK96] and [Ber96].

We make note of the following properties of generating functions and their relationship to twist maps:

Proposition 4 ([Mei92], [Gol01])**.**

1. *If T is an area preserving twist map, it admits a generating function, unique up to an additive constant, given by*

$$G(s_0, s_2) = \int_{\widehat{\gamma}}^{(s_0, s_2)} u_2(\xi, \eta)d\eta - u_0(\xi, \eta)d\eta$$

   where $\widehat{\gamma}$ is an arbitrary path in $S^1 \times S^1$ that ends at (s_0, s_2) (in fact, it can be shown that this integral is path-independent), so that dG is an exact one-form.

2. *If G is C^2, the map T generated by G is always area-preserving. It is a twist map if $\dfrac{\partial^2 G}{\partial s_0 \partial s_2}$ maintains its sign and is always nonzero.*

3. *If G is C^2, u is a constant of motion if and only if $G(s_0, s_2) = g(s_2 - s_0)$ for some function g.*

In the standard billiard setting, the generating function is known to be the negative of the Euclidean (chord) distance between successive collisions with the boundary. In the magnetic billiard settings the generating function also depends upon the area associated with a piece of a typical trajectory, often appearing in the form of a flux term. It is not surprising that in this problem that has elements of both standard and magnetic billiards, that our generating function contains a combination of these elements.

Theorem 1. *Suppose that Ω is a strictly convex set with C^3 boundary $\Gamma(s)$ and that the return map T is a twist map. Then the generating function is*

$$G(s_0, s_2) = -\ell_1 - |\gamma| + \frac{1}{\mu}\mathcal{S}$$

where ℓ_1 is the length of the line segment inside Ω, $|\gamma|$ is the length of the circular arc γ of Larmor radius μ, and $\mathcal{S}$ is the area inside the circular arc γ but outside

Ω.

We prove this in Appendix A.5. However, an interesting property of this generating function (and this problem in general) is as follows: In the high magnetic field limit (i.e. $\mu \to 0$), observe that $|\gamma| \to 0$ and $\frac{1}{\mu}\mathcal{S} \to 0$. This is because $|\gamma| = O(\mu)$ and $\mathcal{S} = O(\mu^2)$. So as $\mu \to 0$, our generating function approaches the standard billiard generating function, and our return map approaches the standard billiard map for billiards inside a convex set.

Repeating another move from [BK96], it may be useful to write G in the form

$$G(s_0, s_2) = \left[-\ell_1 - \frac{1}{\mu}\mathcal{A}\right] + \left[-|\gamma| + \frac{1}{\mu}Area(\mathcal{A} \cup \mathcal{S})\right]$$

$$= E(s_0, s_2) + F_\mu(\chi(s_0, s_2))$$

where $Area(\mathcal{A} \cup \mathcal{S})$ is the area of $\mathcal{A} \cup \mathcal{S}$, $E(s_0, s_2)$ has quantities ℓ_1 and $\mathcal{A}$ which are not dependent upon the magnetic field (see Figure 2.1), and F_μ is dependent up on the magnetic field and can be written as

$$F_\mu(\chi(s_0, s_2)) = -\mu(\chi + \sin(\chi)\cos(\chi)).$$

Or we can write F_μ as a function of ℓ_2, though with caveats:

$$F_\mu(\ell_2(s_0, s_2)) = -\mu \arccos\left(\pm\sqrt{1 - \frac{\ell_2^2}{4\mu^2}}\right) - \pm\frac{\ell_2}{2}\sqrt{1 - \frac{\ell_2^2}{4\mu^2}},$$

where $+$ is used if $0 < \chi \le \frac{\pi}{2}$ and $-$ is used if $\frac{\pi}{2} < \chi < \pi$.

2.3 Periodic Orbits

One particularly useful application of a generating function is in the search of periodic orbits. It will be convenient to lift the periodic variable s from $\mathbb{R}/L\mathbb{Z}$ to $\mathbb{R}$, and will denote the lift of the return map T as $\widehat{T}$.

Definition 3. *The **orbit** of the point (s_0, u_0) is the biinfinite sequence*

$$\{\ldots, (s_{-2}, u_{-2}), (s_0, u_0), (s_2, u_2), \ldots\}$$

where $(s_{2k}, u_{2k}) = \widehat{T}(s_{2k-2}, u_{2k-2})$. Each point is given by successive iterates of $\widehat{T}$.

Lemma 1 ([Gol01]). *Let $\widehat{T}$ be the lift of a twist map T of the annulus and let $G(s_0, s_2)$ be its generating function. There is a one-to-one correspondence between orbits $\{(s_{2k}, u_{2k}) = \widehat{T}^k(s_0, u_0)\}_{k \in \mathbb{Z}}$ of $\widehat{T}$ and sequences $\{s_{2k}\}_{k \in \mathbb{Z}}$ satisfying*

$$\partial_1 G(s_{2k}, s_{2k+2}) + \partial_2 G(s_{2k-2}, s_{2k}) = 0 \qquad \forall k \in \mathbb{Z},$$

where ∂_i denotes partial differentiation with respect to the ith component. The correspondence is given by

$$u_{2k} = -\partial_1 G(s_{2k}, s_{2k+2}).$$

If we define the *n*-point generating function by

$$G^{(n)}(s_0, s_2, \ldots, s_{2n-2}) := G(s_0, s_2) + G(s_2, s_4) + \cdots + G(s_{2n-2}, s_0),$$

often also called the *action* of the sequence of points $\{s_0, s_2, \ldots, s_{2k-2}\}$, then the Critical Action Principle tells us that $\{s_0, s_2, \ldots, s_{2k-2}\}$ is the projection of an orbit segment of $\widehat{T}$ onto the *s*-axis if and only if it is a critical point of $G^{(n)}$ (of

course, restricted to the subspace of sequences $\{w_N, \ldots, w_M\}$ with fixed endpoints, $w_N = s_0$ and $w_M = s_{2n-2}$).

Definition 4. *An* $(\boldsymbol{m}, \boldsymbol{n})$ *periodic orbit is an orbit such that* $s_{2n} = s_0 + mL$, $u_{2n} = u_0$, *and its* **frequency** *(also referred to as the* **rotation number**) *is*

$$\omega = \frac{1}{L} \lim_{k \to \infty} \frac{s_k}{k} = \frac{m}{n}.$$

Hence, if $\widehat{T}$ is iterated n times, the points of an (m, n) periodic orbit will get translated mL times in the s direction. In the annulus, this can be interpreted as wrapping m times around the annulus in n iterates. However, we must note that the integer m does depend upon the lift from T to $\widehat{T}$.

A continuous orientation-preserving homeomorphism of the circle S^1 to itself has a well-defined rotation number, defined modulo 1, when the circle is normalized to have perimeter 1. When a lift to $\mathbb{R}$ of this homeomorphism is chosen, this rotation number is now a real number. By the definition of a twist map, T sends boundary circles to boundary circles, so the lifted homeomorphism has a bottom and top rotation number, ω_- and ω_+. Then the rotation numbers belong to an interval $\mathcal{I}(\widehat{T}) = [\omega_-, \omega_+]$ provided $\omega_- < \omega_+$. In particular, if the map is the identity on the boundary circles then necessarily $\omega_-, \omega_+ \in \mathbb{Z}$.

Proposition 5 ([Gol01]). *A* (m, n) *periodic sequence* $\boldsymbol{s} = \{s_0, s_2, \ldots, s_{2n-2}\}$ *is the* s-*projection of an* (m, n) *periodic orbit if and only if it is a critical point of the periodic action*

$$W_{mn}(s_0, \ldots, s_{2n-2}) := G(s_{2n-2}, s_0 + mL) + \sum_{j=1}^{n-1} G(s_{2j-2}, s_{2j}).$$

Theorems about the existence of periodic orbits for continuous area-preserving twist maps can be attributed to Poincaré and Birkhoff, Aubry, Mather, Meiss, and
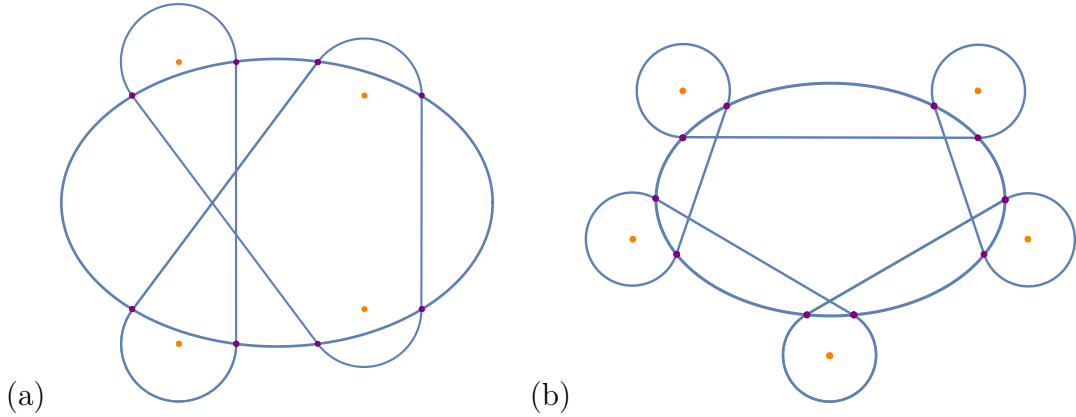
Figure 2.4: (a) A (2,4) periodic orbit for an ellipse with semi-major axis 3, semi-minor axis 2, $\mu = 4/5 < \rho_{min} = 4/3$, and $(s_0, u_0) \approx (1.3796, -0.491598)$; (b) A (4,5) periodic orbit for an ellipse with semi-major axis 3, semi-minor axis 2, $\mu = 1/2 < \rho_{min}$, and $(s_0, u_0) \approx (0, 0.501393)$. The centers of the Larmor circles are marked in orange and the points P_i are in dark purple.

Katok. See [Mei92] for more details. We quote the summary from [BK96], making adjustments for our notation:

1. For every m, n, $\frac{m}{n} \in \mathcal{I}(\widehat{T})$, there is at least one (m, n) periodic orbit which is "maximizing." This means that every finite orbit segment $(s_{2k}, \ldots, s_{2l})$, $2l \geq 2k + 2$ is a global maximum of $\sum_{j=k}^{l-1} G(s_{2j}, s_{2j+2})$. with respect to variations of $s_{2k+2}, \ldots, s_{2l-2}$. In particular, $(s_0, \ldots, s_{2n-2})$ is a global maximum of $G^{(n)}$. If the maximum is nondegenerate, the orbit is hyperbolic.

2. For every m, n, $\frac{m}{n} \in \mathcal{I}(\widehat{T})$, there is at least one (m, n) periodic orbit which is "maximin." This means that the Hessian matrix of $\sum_{j=k}^{l-1} G(s_{2j}, s_{2j+2})$ has one single positive eigenvalue. The orbit is either elliptic or inverse hyperbolic.

3. Every orbit on a rotationally invariant circle is maximizing. For every irrational $\omega \in \mathcal{I}(\widehat{T})$, there is a maximizing quasiperiodic orbit of frequency ω. Its closure is either an invariant circle, or an invariant Cantor set. This

result is in some sense stronger than KAM theory, since it shows the existence of quasiperiodic orbits for twist maps that are not necessarily nearly integrable.

These theorems tell us that the generating function is a powerful tool in the search for and classification of periodic orbits. This provides a lower bound on the number of periodic orbits of period n whose stability can be related to the second derivative of the generating function.

We take a similar approach below, and can apply the Poincaré-Birkhoff Theorem to the map T while making qualitative comments about the behavior of T.

Proposition 6. *Consider the three curvature regimes:*

1. *If $\mu < \rho_{min}$, the function $s_2(s_0, u_0)$ is strictly monotonic in u_0, and hence T is a twist map. The curve $\{T(s_0, u_0) : -1 < u_0 < 1\}$ rotates once around phase space (see Figure 2.5a) with $\lim_{u_0 \to \pm 1} T(s_0, u_0) = (s_0, u_0)$. Therefore $\mathcal{I}(\widehat{T}) = [0, 1]$.*

2. *If $\rho_{min} < \mu < \rho_{max}$, then the map may be discontinuous due to the Larmor circle becoming tangent to the boundary. The function $s_2(s_0, u_0)$ is not necessarily monotonic in u_0 and is not a twist map (see Figure 2.5c). It is still true that $\lim_{u_0 \to 1} T(s_0, u_0) = (s_0, u_0)$, but not necessarily when $u_0 \to -1$.*

3. *If $\rho_{max} < \mu$, then $s_2(s_0, u_0)$ is initially decreasing in u_0 and then begins to increase again (see Figure 2.5e). We still have $\lim_{u_0 \to \pm 1} T(s_0, u_0) = (s_0, u_0)$, which implies that there are exactly two distinct trajectories with equal χ for a given s_0, s_2. Thus we expect $\mathcal{I}(\widehat{T}) \subset [0, 1]$*
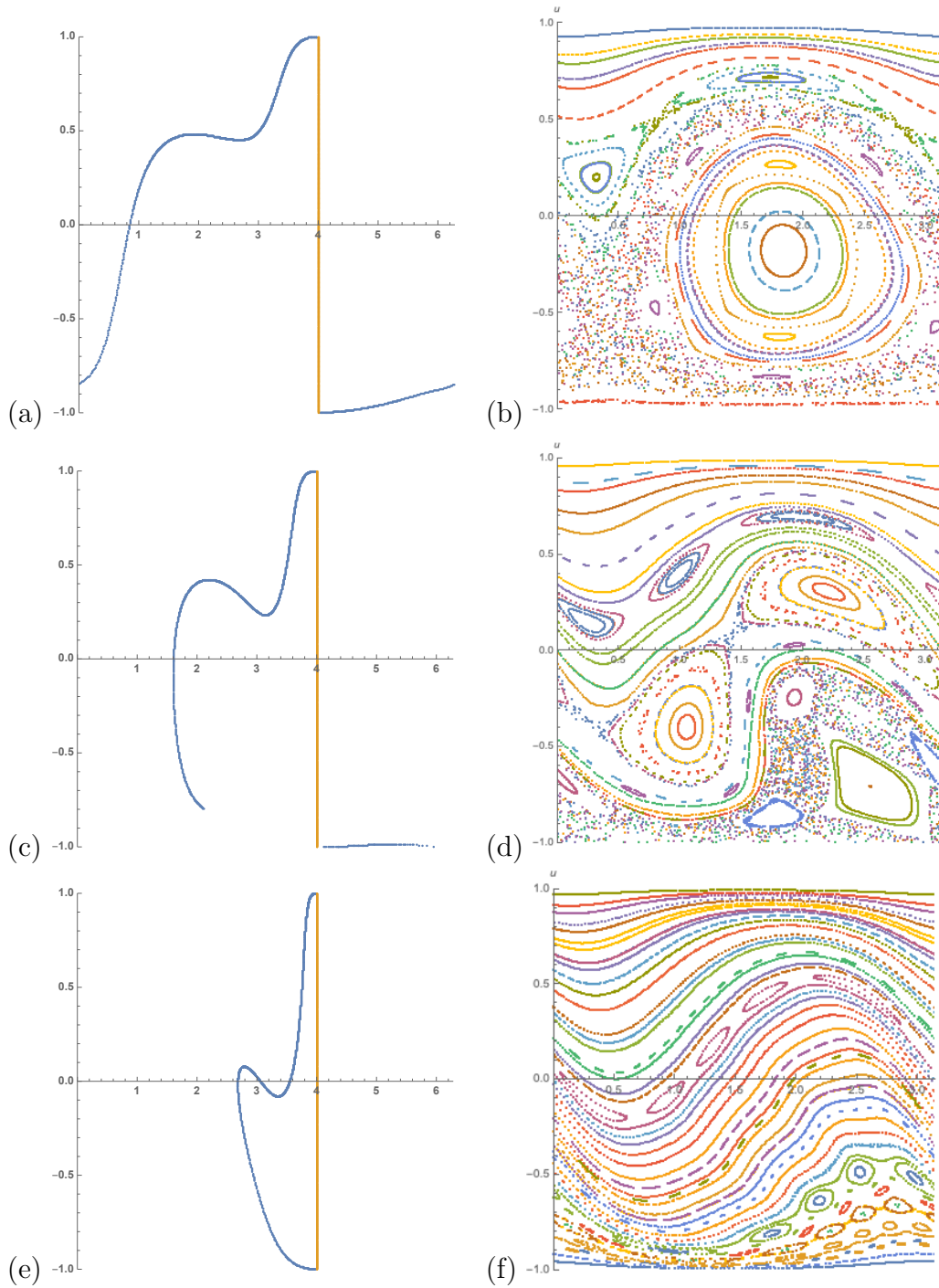
Figure 2.5: Structure of the phase space in the (ϕ, u)-plane for an ellipse where horizontal axis is ϕ, the polar angular parameter used in place of arc length, s. The line $\phi = \phi^*$ is in orange while its image under T is in blue in the left column, $-1 \leq u \leq 1$ for: (a) $\mu < \rho_{min}$; (c) $\rho_{min} < \mu < \rho_{max}$; (e) $\rho_{max} < \mu$. The right column is half of a typical phase portrait, $0 \leq \phi \leq \pi$, of an ellipse for: (b) $\mu < \rho_{min}$; (d) $\rho_{min} < \mu < \rho_{max}$; (f) $\rho_{max} < \mu$.

19

This proposition is very similar to the qualitative behavior of magnetic billiards. In particular, part (1) tells us that for any convex set with smooth boundary and nonvanishing curvature, periodic orbits of every rational frequency $\omega = \frac{m}{n}$ exist, and the earlier summary gives us information about rational and irrational orbits in $\mathcal{I}(\widehat{T})$.

2.4   When $\partial\Omega$ is an Ellipse

We take a quick detour and consider the case when $\partial\Omega$ is an ellipse. Consider the parametrization of $\partial\Omega$ as

$$\boldsymbol{x}(\phi) = (\lambda\cos(\phi), \sin(\phi)), \quad \frac{ds}{d\phi} = C(\phi) = \sqrt{\lambda^2\sin^2(\phi) + \cos^2(\phi)}.$$

Without loss of generality we may assume that the parameter $\lambda \geq 1$. In such a case, $\rho_{min} = \lambda^{-1}$. Consider the points $P_i = \boldsymbol{x}(\phi_i), i = 0, 1, 2$.

Assuming then that $\mu < \rho_{min}$, an important geometric consequence is that $\phi_2 - \phi_1 < \pi$, which simplifies the calculation below. Then T is a twist map and

$$G = -2\sin(\phi_{10}^-)C(\phi_{10}^+) - \frac{1}{\mu}\lambda\left(\phi_{21}^- - \frac{1}{2}\sin(2\phi_{21}^-)\right) + F_\mu(2\sin(\phi_{21}^-)C(\phi_{21}^+))$$

where $\phi_{ab}^\pm = \dfrac{\phi_a \pm \phi_b}{2}$.

There are obvious examples of $(1, 2)$ periodic orbits in the elliptic case, depending upon the lengths of the major and minor axes. These $(1, 2)$ periodic orbits are shaped like the Bunimovich stadium: geometrically, these occur when the centers of the magnetic circular arcs are on the major (resp. minor) axis and the line segment portions of the trajectory are parallel to the major (resp. minor) axis.

In the case that Ω is the unit disk ($\lambda = 1$), we see that $C = 1$ and hence $\phi_2 - \phi_0 = 2\chi$. Another geometric observation is that $\theta_i = \theta$ and χ are both constant, and hence $u_i = u$ is constant. This is because the the diagram in Figure 2.1 is symmetric about the line connecting the center of Ω and the center of the circular arc. This in turn implies that all of our geometric quantities, ℓ_1, ℓ_2, $|\gamma|$, and $\mathcal{S}$ are constant as they only depend upon θ and χ. By Proposition 1,

$$\chi = \theta + \arcsin\left(\frac{\mu \sin(\theta)}{\sqrt{1 + \mu^2 - 2\mu \cos(\theta)}}\right)$$

and the return map is explicitly

$$T(s, u) = (s + 2\chi, u).$$

It is clear that since θ is constant, u is a constant of motion and the system is integrable (in the sense of Liouville).

Further, the simplicity of the return map in the circular case allows us to find periodic orbits directly. Since

$$T(s_0, u_0) = (s_0 + 2\chi, u_0),$$

we see that

$$\widehat{T}^n(s_0, u_0) = (s_0 + 2n\chi, u_0).$$

This means that we will have a (m, n) periodic orbit if and only if $s_0 + 2n\chi = s_0 + 2m\pi$ for some $m \in \mathbb{Z}$, implying χ is a positive rational multiple of π.

21
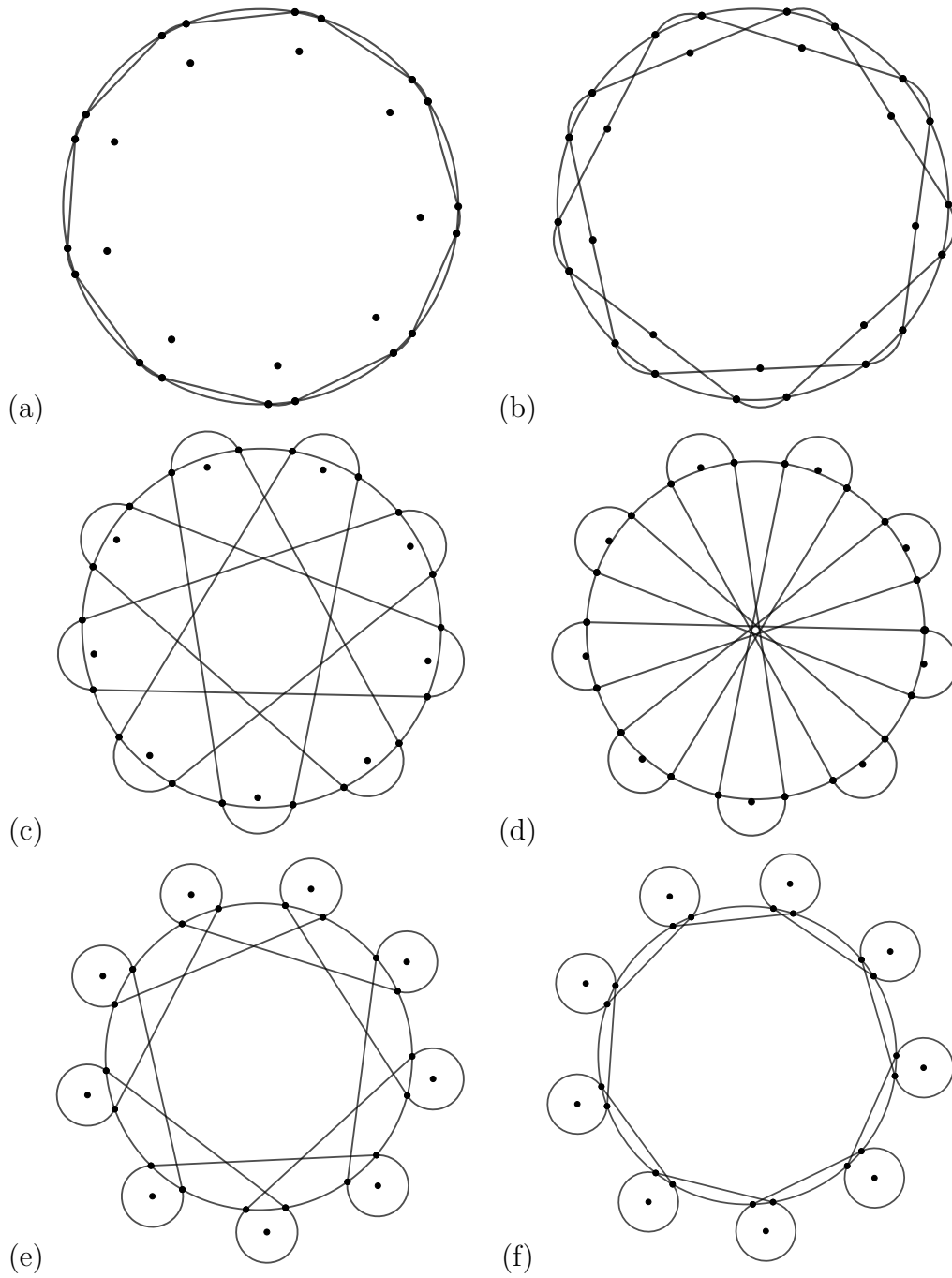
Figure 2.6: Periodic orbits of period 9 in the unit circle with $\mu = \frac{1}{5} < \rho_{min}$:
(a) $(1,9)$ and $(s_0, u_0) \approx (0, -0.96083)$; (b) $(2,9)$ and $(s_0, u_0) \approx (0, -0.84236)$;
(c) $(4,9)$ and $(s_0, u_0) \approx (0, -0.36406)$; (d) $(5,9)$ and $(s_0, u_0) \approx (0, -0.02373)$; (e)
$(7,9)$ and $(s_0, u_0) \approx (0, 0.67713)$; (f) $(8,9)$ and $(s_0, u_0) \approx (0, 0.91404)$. The dots
along the circle are the points P_i while the other dots are the centers of the Larmor
arcs.

Chapter 3

Existence and Nonexistence of Caustics

3.1 Preliminary Results

Definition 5. *Let $\Omega \subset \mathbb{R}^2$ be a strictly convex bounded domain. An **inner convex caustic** is a smooth closed convex curve in Ω with the property that each trajectory that is tangent to it stays tangent to it after each successive reentry. An analogous definition holds for outer caustics which contain Ω.*

In both standard and magnetic billiards, the question of the existence of caustics has been addressed by Lazutkin [Laz73], Berglund and Kunz [BK96], Moser [Mos16], and more in several variants of the standard billiard problem. Trajectories with caustics (the "whispering gallery modes") correspond to invariant curves (a homotopically nontrivial curve) in phase space . Lazutkin had to assume a high degree of differentiability of the boundary in order to guarantee the existence of caustics, though this was later reduced to degree 6 by Douady [Dou82].

In a circle of radius R, elementary geometry shows that all trajectories of the

inverse magnetic billiard have both inner and outer caustics that are circles of radii $r_{inner} = R|\cos(\theta_0)| = R|u_0|$ and $r_{outer} = \mu + \sqrt{R^2 + \mu^2 - 2R\mu\cos(\theta_0)}$, respectively. All of the trajectories in Figure 2.6 have both inner and outer circular caustics.

Our first result in this regard is an inverse magnetic version of Mather's theorem ([Mat82], [MF94]): If a billiard table with a smooth convex boundary curve has a point of vanishing curvature, then the billiard inside the curve has no caustics.

Theorem 2. *If the boundary of the billiard table $\partial\Omega = \Gamma$ has a point of vanishing curvature and $\mu < \rho_{min}$, the inverse magnetic billiard has no interior caustics.*

Proof. By Birkhoff's Theorem ([Bir27]), an invariant curve of an area-preserving twist map is a graph of some function. If our billiard has a caustic, then we have a one-parameter family of chords $P_0 P_1$ to Γ corresponding to points on the invariant curve. The graph property of Birkhoff's Theorem implies that if $P_0^* P_1^*$ is a nearby chord such that P_0^* has moved along Γ in the positive direction from P_0 then P_1^* has moved in the positive direction from P_1 on Γ. These chords must intersect in the interior of Γ, and by the existence of the caustic, must be tangent to the caustic.

Assume an interior caustic $\widetilde{\Gamma}$ exists. The billiard portion of a trajectory forms a chord $P_0 P_1$ tangent to the caustic, moves along its magnetic arc, and reenters Ω to form the next chord P_2, P_3, also tangent to the caustic. Suppose the curvature Γ as P_2 vanishes. Consider an infinitesimally close chord $P_0^* P_1^*$, tangent to the same caustic, as described earlier, along with its next chord $P_2^* P_3^*$. Since the curvature at P_2 vanishes, the tangent line at P_2^* is, in the linear approximation, the same as the one at P_2. Let θ_2 and θ_2^* be the angle between the linear approximation and the chords $P_2 P_3$ and $P_2^* P_3^*$, respectively.

There are three geometrically distinct cases. If $\chi < \frac{\pi}{2}$, then $\theta_2 > \theta_2^*$, and so

the chords $P_2 P_3$ and $P_2^* P_3^*$ will not intersect in the interior of Γ, a contradiction. See Figure 3.1. Similarly, if $\chi > \frac{\pi}{2}$, $\theta_2 > \theta_2^*$. And if $\chi = \frac{\pi}{2}$, then the chords $P_2 P_3$ and $P_2^* P_3^*$ are parallel and will not intersect.
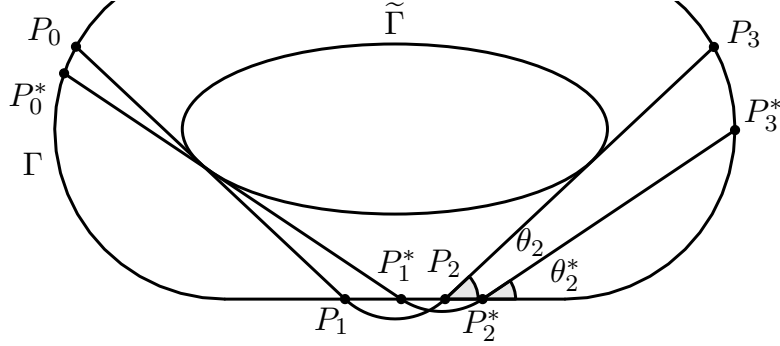
Figure 3.1: Picture of the proof of the nonexistence of caustics if the boundary has a point of vanishing curvature.

$\square$

To better understand the nature of caustics in this inverse magnetic billiard setting, we seek to understand the maps T_1 and T_2 near the boundary, as they show qualitatively different behavior. We also make the temporary adjustment to the maps T, T_1, and T_2 so they are defined on the annulus $\mathbb{R}/L\mathbb{Z} \times [0, \pi]$ so the second variable is θ instead of u. Recall a calculation of Lazutkin:

Proposition 7 ([Laz73]). *The billiard map T_1 admits a Taylor expansion for θ_i near 0:*

$$s_{i+1}(s_i, \theta_i) = s_i + a_1(s_i)\theta_i + a_2(s_i)\theta_i^2 + O(\theta_i^3) \mod L$$

$$\theta_{i+1}(s_i, \theta_i) = b_1(s)\theta_i + b_2(s_i)\theta_i^2 + O(\theta_i^3)$$

where, omitting the dependence upon s_i,

$$a_1 = 2\rho = \frac{2}{\kappa}$$

$$a_2 = \frac{4}{3}\rho\rho' = -\frac{4}{3}\frac{\kappa'}{\kappa^3}$$

$$b_1 = 1$$

$$b_2 = -\frac{2}{3}\rho' = \frac{2}{3}\frac{\kappa'}{\kappa^2}.$$

Writing $\theta_i = \pi - \eta_i$ with η_i near 0,

$$s_{i+1}(s_i, \eta_i) = s_i - a_1(s_i)\eta_i + a_2(s_i)\eta_i^2 + O(\eta_i^3) \mod L$$

$$\eta_{i+1}(s_i, \eta_i) = b_1(s)\eta_i - b_2(s_i)\eta_i^2 + O(\eta_i^3).$$

In fact, the coefficients for the Taylor expansion are known up to fourth order. We will only need the second order expansion for our purposes.

We seek a similar expansion for our outer magnetic billiard map. In [BK96], Taylor expansions for the inner magnetic billiard map T_2^* are found up to first order using a different technique. For the sake of comparison with our result, we state their conclusion below.

Proposition 8 ([BK96])**.** *The inner magnetic billiard map T_2^* is of the form*

$$s_{i+1} = s_i - \frac{2\mu\sin(\theta_i)}{1 - \mu\kappa_i\cos(\theta_i)} + o(\sin(\theta_i)) \mod L$$

$$\theta_{i+1} = \theta_i + o(\sin(\theta_i)).$$

Therefore near $u = -1$, the map is of the form

$$s_{i+1} = s_i - \frac{2\mu}{1 - \mu\kappa_i}\theta_i + o(\theta_i) \mod L$$

$$\theta_{i+1} = \theta_i + o(\theta_i)$$

and near $u = 1$, writing $\theta_i = \pi - \eta_i$ the map is of the form

$$s_{i+1} = s_i - \frac{2\mu}{1 + \mu\kappa_i}\eta_i + o(\eta_i) \mod L$$

$$\eta_{i+1} = \eta_i + o(\eta_i).$$

Through variable changes, this map is used to show the existence of caustics in inner magnetic billiards for three special cases by citing a version of the KAM theorems ([Mos16], [Dou82]). Our goal is to produce a similar result to that of [BK96] and [Laz73].

3.2 Mimicking the Approach of Berglund and Kunz

We can investigate the behavior of the outer magnetic billiard map T_2 using the same techniques in [BK96], and ultimately learn about T. For a nonzero magnetic field near the boundary, we will be able to apply KAM theorems to show the existence of invariant curves.

Recall our construction from Section 1.1 and Appendix A.2. Let $z(s) = X(s)+$

$iY(s)$, $z_i = z(z_i)$, $\tau_i = \tau(s_i)$. Then

$$z_2 - z_1 = \int_{s_1}^{s_2} e^{i\tau(s)}\, ds = \int_{\tau_1}^{\tau_2} \rho(\tau) e^{i\tau}\, d\tau.$$

The points z_1, z_2 also are on the arc of a magnetic trajectory, which have tangent directions $\tau_1 - \theta_1$ and $\tau_2 + \theta_2$, respectively. Thus

$$z_2 - z_1 = \frac{\mu}{i}\left(e^{i(\tau_2+\theta_2)} - e^{i(\tau_1-\theta_1)}\right).$$

Define $A = e^{-i\tau_1}(z_2 - z_1)$ and $\delta = (\tau_2 - \tau_1) + (\theta_2 - \theta_1)$. Then we can write the previous expression as

$$A - \frac{\mu}{i} e^{i\theta_1}(e^{i\delta} - 1) = 2\mu \sin(\theta_1).$$

Expanding the left side and equating real and imaginary parts, we have the system

$$\frac{\operatorname{Re}(A)}{\sin(\theta_1)} - \mu(\cos(\delta) - 1) - \mu\cos(\theta_1)\frac{\sin(\delta)}{\sin(\theta_1)} = 2\mu$$

$$\frac{\operatorname{Im}(A)}{\sin^2(\theta_1)} + \mu\cos(\theta_1)\frac{\cos(\delta) - 1}{\sin^2(\theta_1)} - \mu\frac{\sin(\delta)}{\sin(\theta_1)} = 0.$$

If the boundary is C^k, then this is a system of C^{k-1} equations in the variables $s_1, s_2, \theta_1, \theta_2$ that we would like to solve for s_2, θ_2. Writing $s_2 = s_1 + \mu\sin(\theta_1)\sigma$ and $\theta_2 = \theta_1 + \mu\sin(\theta_1)\gamma$, we find that

$$\delta = \mu\sin(\theta_1)\left(\gamma + \sigma\kappa_1\right) + O(\mu^2\sin^2(\theta_1))$$

$$A = \mu\sin(\theta_1)\sigma + \frac{i}{2}\mu^2\sin^2(\theta_1)\sigma^2\kappa_1 + O(\mu^3\sin^3(\theta_1)).$$

Combining these two systems of equations leads to the system

$$\sigma - \mu \cos(\theta_1)\,(\gamma + \sigma\kappa_1) + O(\sin(\theta_1)) = 2$$

$$\sigma^2 \kappa_1 - 2(\gamma + \sigma\kappa_1) - \mu \cos(\theta_1)(\gamma + \sigma\kappa_1)^2 + O(\sin(\theta_1)) = 0,$$

which has solution

$$\sigma(s_1, \theta_1, \mu) = \frac{2}{1 - \mu\kappa_1 \cos(\theta_1)} + O(\sin(\theta_1))$$

$$\gamma(s_1, \theta_1, \mu) = O(\sin(\theta_1)).$$

The Jacobian of this system evaluated at this solution is $-2 + O(\sin(\theta_1))$, so the implicit function theorem implies that, provided $\sin(\theta_1)$ is sufficiently small, the map T_2 can be written in a simple form. We summarize this result in the following theorem.

Theorem 3. *If the boundary $\partial\Omega$ is C^k, the outer magnetic billiard map T_2 is C^{k-1} for small $\sin(\theta_1)$ and has the form*

$$s_2 = s_1 + \frac{2\mu \sin(\theta_1)}{1 - \mu\kappa_1 \cos(\theta_1)} + o(\sin(\theta_1)) \quad \mathrm{mod}\ L$$

$$\theta_2 = \theta_1 + o(\sin(\theta_1)).$$

Therefore, near $u = -1$, the map is of the form

$$s_2 = s_1 + \frac{2\mu}{1 - \mu\kappa_1}\theta_1 + o(\theta_1) \quad \mathrm{mod}\ L$$

$$\theta_2 = \theta_1 + o(\theta_1)$$

and near $u = 1$, writing $\theta_i = \pi - \eta_i$ the map is of the form

$$s_2 = s_1 + \frac{2\mu}{1 + \mu\kappa_1}\eta_1 + o(\eta_1) \mod L$$

$$\eta_2 = \eta_1 + o(\eta_1).$$

This expression for the outer magnetic billiard map is unsurprisingly very similar to the form of the inner magnetic billiard map in Proposition 8.

We must be cautious as there are two properties we must check with regards to the map above. First, the map must be well-defined (so the denominators may not vanish). This is only an issue when $\theta \ll 1$. The second is that the outer magnetic billiard map must denote the *correct* intersection of the magnetic arc with the boundary of our billiard table. This is only an issue if a magnetic arc intersects the boundary in more than two places.

Definition 6. *A closed plane C^2 curve is said to have the **μ-intersection** property for some $\mu > 0$ if any circle of radius μ intersects it at most twice.*

However, a sufficient condition for the μ-intersection property to be satisfied is for either $\mu < \rho_{min}$ or $\rho_{max} < \mu$ (Corollary to Lemma 3 in Appendix D of [BK96]). When satisfied, there is a one-to-one correspondence between inner magnetic billiard trajectories and outer magnetic billiard trajectories. For every outer magnetic arc there is a "dual trajectory" that is the complementary arc which completes the circle, which can be interpreted as an inner magnetic billiard map with no change to our magnetic field convention. See Figure 3.2.

Therefore determining the correct intersection point from our map is only an issue when $\rho_{min} < \mu < \rho_{max}$, as a Larmor circle in this case may intersect the table in more than two places.

If we consider the three curvature regimes, we notice the following:
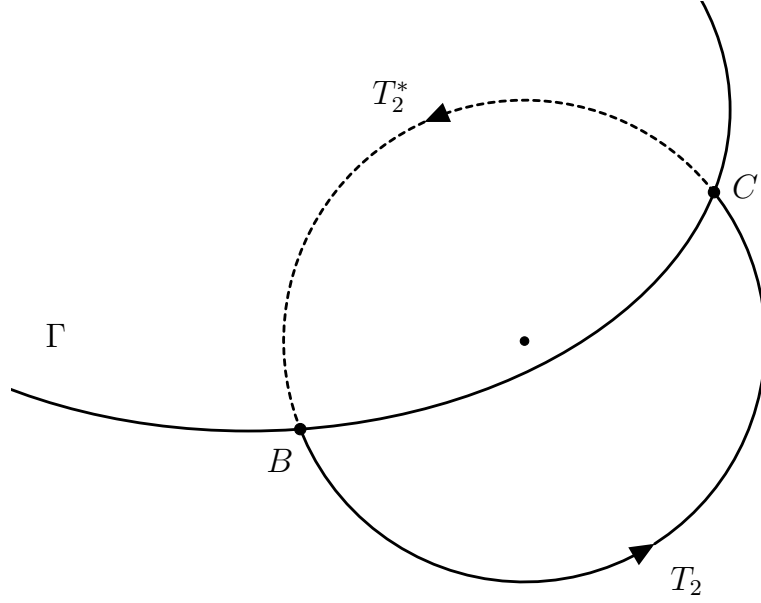
Figure 3.2: The duality of the magnetic billiard map: every inner magnetic billiard trajectory has a corresponding outer magnetic billiard trajectory, provided the μ-intersection property is satisfied.

1. If $\mu < \rho_{min}$, then $\mu\kappa(s) \leq \mu\kappa_{max} < 1$, so $0 < 1 - \mu\kappa(s)$ for all s;

2. If $\rho_{min} < \mu < \rho_{max}$, then $\frac{\kappa_{min}}{\kappa_{max}} < \mu\kappa_{min} < 1 < \mu\kappa_{max} < \frac{\kappa_{max}}{\kappa_{min}}$;

3. If $\rho_{max} < \mu$, then $1 < \kappa_{min}\mu \leq \kappa(s)\mu$, so $1 - \mu\kappa(s) < 0$ for all s.

The denominators of the coefficients in the theorem above are well-defined in cases (1) and (3), but potentially not defined in case (2).

As an immediate corollary, using the known expansion of T_1, we have the following:

Corollary 3. *The inverse magnetic billiard map T admits the following Taylor expansion for θ_i near 0:*

$$s_{i+2} = s_i + \frac{2}{\kappa_i(1 - \mu\kappa_i)}\theta_i + O(\theta_i^2) \quad \mod L$$

$$\theta_{i+2} = \theta_i + O(\theta_i^2)$$

31

where we have omitted the dependence upon s_i and that $\kappa_i := \kappa(s_i) \approx \kappa(s_{i+1})$.

For $\theta_i = \pi - \eta_i$ with η_i near 0, the map T admits the Taylor expansion

$$s_{i+2} = s_i - \frac{2}{\kappa_i(1 + \mu\kappa_i)}\eta_i + O(\eta_i^2) \quad \mathrm{mod}\ L$$

$$\eta_{i+2} = \eta_i + O(\eta_i^2).$$

First we observe that both versions of this map are not well-defined if the curvature is allowed to vanish, which matches up with our version of Mather's result. Further, consider the two limiting cases of μ: if $\mu \to \infty$, the map T limits to $s_2 = s_0 + o(\theta_0^2)$, and $\theta_2 = \theta_0 + o(\theta_0^2)$ which the identity map to first order; And if $\mu \to 0^+$, the map T limits to $s_2 = s_0 + \frac{2}{\kappa_0}\theta_0 + o(\theta_0^2)$, which is the standard billiard map to first order. This is consistent with our geometric observations via the generating function in Section 2.2.

We may now make comments about the maps above in the style of [BK96].

1. Near $u = -1$, the map T has the form

$$s_{i+2} = s_i + \frac{2}{\kappa_i(1 - \mu\kappa_i)}\theta_i + O(\theta_i^2) \quad \mathrm{mod}\ L$$

$$\theta_{i+2} = \theta_i + O(\theta_i^2).$$

We have already observed that the denominator will not vanish in two cases:

- If $\mu < \rho_{min}$, then we make the change of variables $\varphi_i = s_i - \mu\tau_i$ and $r_i = 2\rho_i\theta_i$ to make the map of the form

$$\varphi_2 = \varphi_0 + r_0 + o(r_0^2) \quad \mathrm{mod}\ L - 2\pi\mu$$

32

$$r_2 = r_0 + o(r_0^2).$$

This corresponds to the correct intersection of the magnetic arc with the boundary, as this trajectory corresponds to a small billiard chord forward plus a small skip forward along the boundary from the outside.

- if $\rho_{max} < \mu$, then we make the change of variables $\varphi_i = \mu\tau_i - s_i$ and $r_i = 2\rho_i\theta_i$ to make the map of the form

$$\varphi_2 = \varphi_0 - r_0 + o(r_0^2) \mod 2\pi\mu - L$$
$$r_2 = r_0 + o(r_0^2).$$

Again, this is the correct intersection with the boundary, because a large magnetic arc will reenter Ω "behind" its exit point.

2. Near $u = 1$, the map T has the form

$$s_{i+2} = s_i - \frac{2}{\kappa_i(1 + \mu\kappa_i)}\eta_i + O(\eta_i^2) \mod L$$
$$\eta_{i+2} = \eta_i + O(\eta_i^2)$$

where we have written $\theta_i = \pi - \eta_i$. Observe that the denominator can never vanish, so this approximation is valid for all three curvature regimes. Moreover, this map can be understood as a short interior billiard chord backwards followed by most of a circular magnetic arc forwards, ultimately resulting in traveling a small distance backwards. The change of variables $\varphi_i = s_i + \mu\tau_i$ and $r_i = 2\rho_i\eta_i$ turns the map into

$$\varphi_2 = \varphi_0 - r_0 + o(r_0^2) \mod L + 2\pi\mu$$

$$r_2 = r_0 + o(r_0^2).$$

Each of these three maps can be interpreted via KAM theorems ([Dou82], pg. III-8 or [Mos16] pg. 52).

Definition 7. *Let $\sigma \in \mathbb{R}$. We say σ satisfies the **Diophantine condition** if for every $\frac{p}{q} \in \mathbb{Q}$, there exists $\gamma, \nu \in \mathbb{R}^+$ such that*

$$\left| \sigma - \frac{p}{q} \right| \geq \gamma q^{-\nu}.$$

Theorem 4. *Consider the inverse magnetic billiard in a strictly convex set Ω with C^k boundary, $k \geq 6$. Consider the following cases:*

1. *if $0 < \mu < \rho_{min}$, define $\zeta = \theta$, $M = L - 2\pi\mu$, and $\lambda = 1$;*

2. *if $\rho_{max} < \mu < \infty$, define $\zeta = \theta$, $M = 2\pi\mu - L$, $\lambda = -1$;*

3. *or if $0 < \mu < \infty$, define $\zeta = \pi - \theta$, $M = L + 2\pi\mu$, $\lambda = -1$.*

Then there exists $\epsilon > 0$ depending upon μ and k with the following significance: if $\omega \in [0, \epsilon)$ and satisfies the Diophantine condition, then there is an invariant curve of the form

$$s = \xi + V(\xi)$$
$$\zeta = \frac{\omega}{2\mu} + U(\xi),$$

where $U, V \in C^1$, $V(\xi + M) = V(\xi) + L - M$, $U(\xi + M) = U(\xi)$. The induced map on this curve has the form

$$\xi \mapsto \xi + \lambda\omega.$$

34
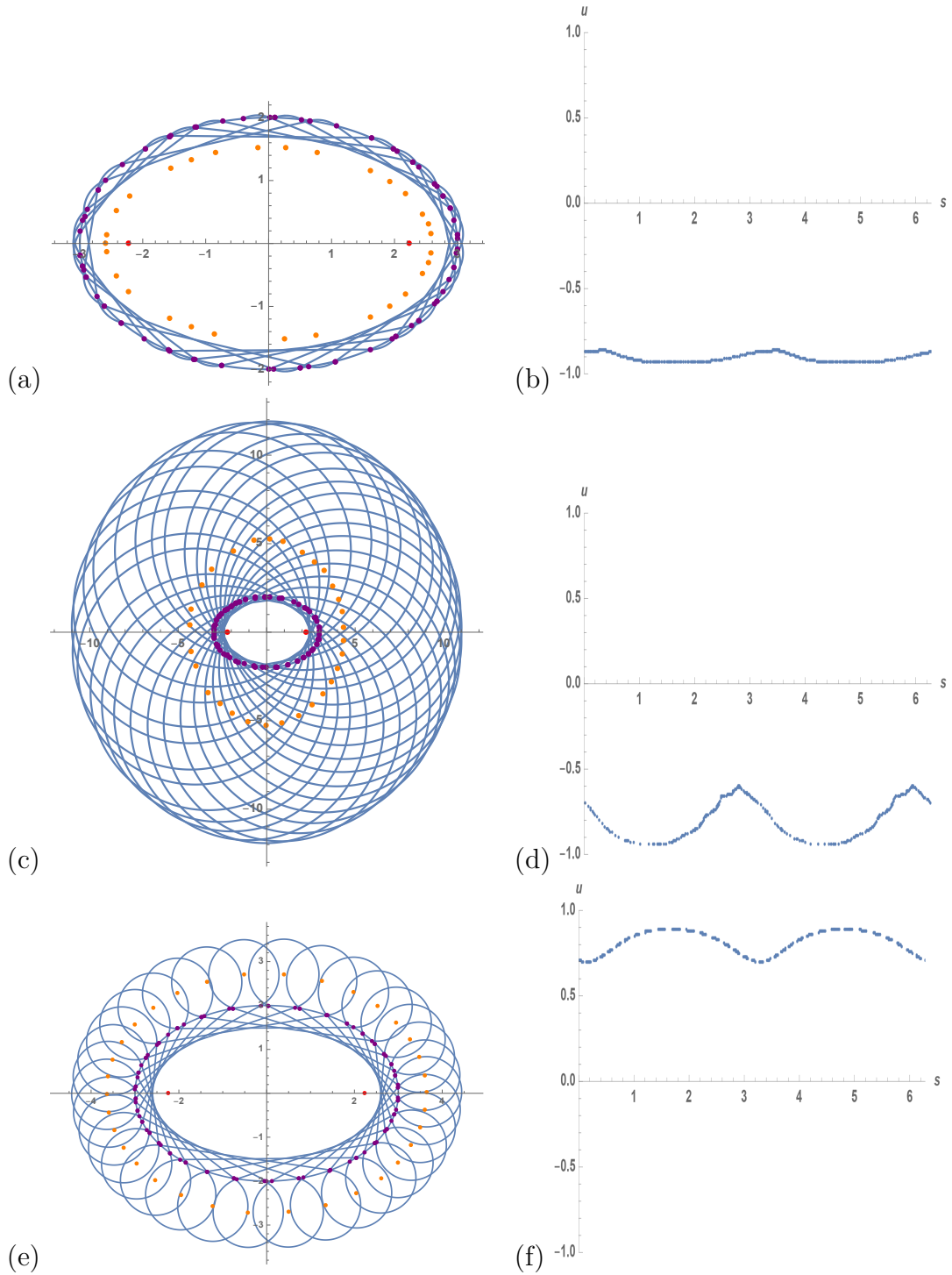
Figure 3.3: Caustics in an ellipse for the three valid regimes: (a) near $u = -1$ and $\mu < \rho_{min}$; (c) near $u = -1$ and $\rho_{max} < \mu$; (e) near $u = 1$; and their accompanying invariant curves in the (ϕ, u)-plane, (b), (d), (e), respectively. The centers of the Larmor circles are marked in orange, the foci of the ellipse are in red, and the points P_i are in dark purple.

35

Similarly to the case of inner magnetic billiards, our theorem confirms the existence of invariant curves in three cases (see Figure 3.3):

1. Near $u = -1$, $\theta \approx 0$ in a strong magnetic field, $\mu < \rho_{min}$. These correspond to short billiard chords plus short magnetic arcs, keeping the particle's trajectory near the boundary.

2. Near $u = -1$, $\theta \approx 0$ in a weak magnetic field, $\rho_{max} < \mu < \infty$. These correspond to short billiard chords followed by long magnetic arcs encompassing Ω and reentering behind the original starting point, still near the boundary.

3. Near $u = 1$, $\theta \approx \pi$ for all values of the magnetic field. These correspond to backwards billiard chords followed by most of a magnetic arc, reentering close to the starting point and staying near the boundary.

This approach does not give us any indication of the behavior of the map for the intermediate curvature regime, $\rho_{min} < \mu < \rho_{max}$ near $u = -1$. While numerically we do not observe any invariant curves in this region in this case, we do not have definitive proof. This is also the case in inner magnetic billiards. Moreover, our theorem also indicates that, provided we have a sufficiently smooth strictly convex boundary (at least C^6), inverse magnetic billiards are not ergodic.

3.3   A Lazutkin-Motivated Approach

In his 1973 paper, Lazutkin [Laz73] uses a fourth-order Taylor expansion of the billiard map together with a theorem of his own to prove the billiard map T_1 can be transformed into a perturbation of an integrable map

$$x_1 = x_0 + y_0 + O(y^3)$$

$$y_1 = y_0 + O(y^4)$$

where the new coordinates (x, y) are called *Lazutkin coordinates*. He used these coordinates as follows: By a KAM Theorem (of Moser [Mos62]) this implies the existence of a positive measure set of caustics accumulating near the boundary corresponding to the existence of KAM invariant curves of a particular form, provided the boundary was sufficiently smooth. The technique of Lazutkin for smooth boundary, and later for an analytic boundary in [MRRTS16], has been generalized to an abstract setting in Appendix A of [dSKW17] and the appendices of [KZ18]. This *Lazutkin normal form* is a variable change by constructing power series of x and y in the map above to arbitrary order, y^N. Notably, the construction of the Lazutkin normal form requires the map T is a twist map, so we will now assume that $\mu < \rho_{min}$.

To that end, we intend to do the same through some explicit calculations.

Proposition 9. *The outer magnetic billiard map T_2 admits a Taylor expansion for θ_i near 0:*

$$s_{i+1}(s_i, \theta_i) = s_i + c_1(s_i)\theta_i + c_2(s_i)\theta_i^2 + O(\theta_i^3) \mod L$$

$$\theta_{i+1}(s_i, \theta_i) = d_1(s_i)\theta_i + d_2(s_i)\theta_i^2 + O(\theta_i^3)$$

where, omitting the dependence upon s_i and writing $\kappa := \kappa(s_i) = \rho(s_i)^{-1} =: \rho^{-1}$,

$$c_1 = \frac{2\mu}{1 - \mu\kappa} = \frac{2\mu\rho}{\rho - \mu}$$

$$c_2 = \frac{2\mu^2 \kappa'}{3(1 - \mu\kappa)^2} = -\frac{2\mu^2 \rho'}{3(\rho - \mu)^2}$$

$$d_1 = 1$$

$$d_2 = -\frac{\mu\kappa'}{3(1 - \mu\kappa)} = \frac{\mu\rho'}{3\rho(\rho - \mu)}.$$

For $\theta_i = \pi - \eta_i$ with η_i near 0, the map T_2 admits the Taylor expansion:

$$s_{i+1}(s_i, \eta_i) = s_i - e_1(s_i)\eta_i + e_2(s)\eta_i^2 + O(\eta_i^3) \mod L$$

$$\eta_{i+1}(s_i, \eta_i) = f_1(s_i)\eta_i - f_2(s_i)\eta_i^2 + O(\eta_i^3)$$

where, omitting the dependence upon s_i and writing $\kappa := \kappa(s_i) = \rho(s_i)^{-1} =: \rho^{-1}$,

$$e_1 = -\frac{2\mu}{1 + \mu\kappa} = -\frac{2\mu\rho}{\rho + \mu}$$

$$e_2 = \frac{2\mu^2\kappa'}{3(1 + \mu\kappa)^2} = -\frac{2\mu^2\rho'}{3(\rho + \mu)^2}$$

$$f_1 = 1$$

$$f_2 = \frac{\mu\kappa'}{3(1 + \mu\kappa)} = -\frac{\mu\rho'}{3\rho(\rho + \mu)}.$$

See Appendix A.6 for the proof and an indication of how to compute higher order terms. As an immediate corollary, we have Taylor expansions for T through function composition.

Corollary 4. *The inverse magnetic billiard map T admits the following Taylor expansion for θ_i near 0:*

$$s_{i+2}(s_i, \theta_i) = s_i + g_1(s_i)\theta_i + g_2(s)\theta_i^2 + O(\theta_i^9) \mod L$$

$$\theta_{i+2}(s_i, \theta_i) = h_1(s_i)\theta_i + h_2(s_i)\theta_i^2 + O(\theta_i^9)$$

where, omitting the dependence upon s_i and assuming that $\kappa := \kappa(s_i) \approx \kappa(s_{i+1})$,

$$g_1 = \frac{2}{\kappa(1 - \mu\kappa)} = \frac{2\rho^2}{\rho - \mu}$$

$$g_2 = \frac{2\kappa'\left(\kappa^3\mu^2 - 4\kappa^2\mu^2 + 6\kappa\mu - 2\right)}{3\kappa^3(1 - \mu\kappa)^2} = \frac{2\rho'\left(\mu^2(4\rho - 1) - 6\mu\rho^2 + 2\rho^3\right)}{3(\rho - \mu)^2}$$

$$h_1 = 1$$

$$h_2 = \frac{\kappa'\left(2 - 2\kappa\mu - \kappa^2\mu\right)}{3\kappa^2(1 - \mu\kappa)} = \frac{\rho'(2\mu\rho + \mu - 2\rho^2)}{3\rho(\rho - \mu)}.$$

For $\theta_i = \pi - \eta_i$ with η_i near 0, the map T admits the Taylor expansion:

$$s_{i+2}(s_i, \eta_i) = s_i + j_1(s_i)\eta_i + j_2(s)\eta_i^2 + O(\eta_i^3) \quad \mod L$$

$$\eta_{i+2}(s_i, \eta_i) = k_1(s_i)\eta_i + k_2(s_i)\eta_i^2 + O(\eta_i^3)$$

where, omitting the dependence upon s_i and assuming that $\kappa := \kappa(s_i) \approx \kappa(s_{i+1})$,

$$j_1 = -\frac{2}{\kappa(1 + \mu\kappa)} = -\frac{2\rho^2}{\rho + \mu}$$

$$j_2 = \frac{2\kappa'\left(\kappa^3\mu^2 - 4\kappa^2\mu^2 - 6\kappa\mu - 2\right)}{3\kappa^3(\kappa\mu + 1)^2} = \frac{2\rho'\left(\mu^2(4\rho - 1) + 6\mu\rho^2 + 2\rho^3\right)}{3(\mu + \rho)^2}$$

$$k_1 = 1$$

$$k_2 = -\frac{\kappa'(\kappa^2\mu + 2\kappa\mu + 2)}{3\kappa^2(1 + \kappa\mu)} = \frac{\rho'(2\rho^2 + 2\rho\mu + \mu)}{3\rho(\rho + \mu)}.$$

Let $(s^+, \theta^+) := T(s, \theta)$ and $(s^-, \theta^-) := T^{-1}(s, \theta)$. To understand the preimage of the point (s, θ), interpret $T^{-1} = (T_2 \circ T_1)^{-1} = T_1^{-1} \circ T_2^{-1}$. Because of the standard billiard reflection law, $T_1^{-1}(s, \theta) = T_1(s, \pi - \theta)$ for which we already have an expression.

For T_2^{-1}, from our earlier observation, we know that if the μ-intersection property is satisfied, there is a one-to-one correspondence between inner- and outer-magnetic billiard trajectories. To that end, we can treat T_2^{-1} as T_2^*, the inner magnetic billiard map.

Proposition 10. *The inner magnetic billiard map T_2^* admits a Taylor expansion*

for θ_i near 0:

$$s_{i+1}(s_i, \theta_i) = s_i + l_1(s_i)\theta_i + l_2(s_i)\theta_i^2 + O(\theta_i^3) \pmod L$$

$$\theta_{i+1}(s_i, \theta_i) = m_1(s_i)\theta_i + m_2(s_i)\theta_i^2 + O(\theta_i^3)$$

where, omitting the dependence upon s_i,

$$l_1 = -\frac{2\mu}{1 - \mu\kappa} = -\frac{2\mu\rho}{\rho - \mu}$$

$$l_2 = -\frac{2\mu^2\kappa'}{3(1 - \mu\kappa)^2} = \frac{2\mu^2\rho'}{3(\rho - \mu)^2}$$

$$m_1 = 1$$

$$m_2 = -\frac{\mu\kappa'}{3(1 - \mu\kappa)} = \frac{\mu\rho'}{3\rho(\rho - \mu)}.$$

For $\theta_i = \pi - \eta_i$ with η_i near 0, the map T_2^* admits the Taylor expansion:

$$s_{i+1}(s_i, \eta_i) = s_i + n_1(s_i)\eta_i + n_2(s)\eta_i^2 + O(\eta_i^3) \pmod L$$

$$\eta_{i+1}(s_i, \eta_i) = p_1(s_i)\eta_i + p_2(s_i)\eta_i^2 + O(\eta_i^3)$$

where, omitting the dependence upon s_i,

$$n_1 = \frac{2\mu}{1 + \mu\kappa} = \frac{2\mu\rho}{\rho + \mu}$$

$$n_2 = -\frac{2\mu^2\kappa'}{3(1 + \mu\kappa)^2} = \frac{2\mu^2\rho'}{3(\rho + \mu)^2}$$

$$p_1 = 1$$

$$p_2 = \frac{\mu\kappa'}{3(1 + \mu\kappa)} = -\frac{\mu\rho'}{3\rho(\rho + \mu)}.$$

The proof is similar to that of the proof of Proposition 9 given in Appendix A.6. Of note, this Taylor expansion of T_2^* agrees with the result of Theorem 3 but

includes higher order terms.

Corollary 5. *The preimage of the inverse magnetic billiard map T^{-1} admits the following Taylor expansion for θ_i near 0:*

$$s_{i+2}(s_i, \theta_i) = s_i + q_1(s_i)\theta_i + q_2(s)\theta_i^2 + O(\theta_i^9) \mod L$$

$$\theta_{i+2}(s_i, \theta_i) = r_1(s_i)\theta_i + r_2(s_i)\theta_i^2 + O(\theta_i^9)$$

where, omitting the dependence upon s_i and assuming that $\kappa := \kappa(s_i) \approx \kappa(s_{i+1})$,

$$q_1 = -\frac{2}{\kappa(1 - \mu\kappa)} = -\frac{2\rho^2}{\rho - \mu}$$

$$q_2 = -\frac{2\kappa'\left(2\kappa^3\mu^2 + \kappa^2\mu(2\mu - 1) - 4\kappa\mu + 2\right)}{3\kappa^3(1 - \mu\kappa)^2} = \frac{2\rho'\left(2\mu^2(\rho + 1) - \mu(4\rho + 1)\rho + 2\rho^3\right)}{3(\rho - \mu)^2}$$

$$r_1 = 1$$

$$r_2 = \frac{\kappa'\left(-\kappa^2\mu + 2\kappa\mu - 2\right)}{3\kappa^2(1 - \mu\kappa)} = \frac{\rho'\left(-2\mu\rho + \mu + 2\rho^2\right)}{3\rho(\rho - \mu)}.$$

For $\theta_i = \pi - \eta_i$ with η_i near 0, the map T admits the Taylor expansion:

$$s_{i+2}(s_i, \eta_i) = s_i + t_1(s_i)\eta_i + t_2(s)\eta_i^2 + O(\eta_i^3) \mod L$$

$$\eta_{i+2}(s_i, \eta_i) = v_1(s_i)\eta_i + v_2(s_i)\eta_i^2 + O(\eta_i^3)$$

where, omitting the dependence upon s_i and assuming that $\kappa := \kappa(s_i) \approx \kappa(s_{i+1})$,

$$t_1 = \frac{2}{\kappa(1 + \mu\kappa)} = \frac{2\rho^2}{\rho + \mu}$$

$$t_2 = -\frac{2\kappa'\left(2\kappa^3\mu^2 + \kappa^2\mu(2\mu + 1) + 4\kappa\mu + 2\right)}{3\kappa^3(1 + \mu\kappa)^2} = \frac{2\rho'\left(2\mu^2(\rho + 1) + \mu(4\rho + 1)\rho + 2\rho^3\right)}{3(\rho + \mu)^2},$$

$$v_1 = 1$$

$$v_2 = \frac{\kappa'\left(-\kappa^2\mu + 2\kappa\mu + 2\right)}{3\kappa^2(1 + \mu\kappa)} = \frac{\rho'\left(-2\mu\rho + \mu - 2\rho^2\right)}{3\rho(\rho + \mu)}.$$

Using the above expansions, we construct the corresponding Lazutkin coordi-
nates. Consider the formal coordinate change given by assuming x and y are of
the form

$$x = X_0(s, \theta) := F_0(s) + G_0(s)\theta^2 + O(\theta^4)$$

$$y = Y_0(s, \theta) := X_0(s, \theta) - X_0(s^-, \theta^-)$$

where F_0 and G_0 are functions to be determined. In particular, we must solve

$$K_0(s, \theta) := Y_0^+ - Y_0 = X_0(s^+, \theta^+) - 2X_0(s, \theta) + X_0(s^-, \theta^-) = O(\theta^4).$$

Expand the left-hand side of this equation near $\theta = 0$. Omitting the dependence
upon s, we get

$$K_0(s, \theta) = \left[\frac{2\left(6\rho^4 F_0''(s) + \rho' F_0'(s)\left(\mu^2(6\rho + 1) - \mu(10\rho + 1)\rho + 4\rho^3\right)\right)}{3(\rho - \mu)^2} \right] \theta^2 +$$
$$\left[\frac{4\mu\rho'\left(\rho^3 F_0''(s)\left(\mu(2\rho - 3) - 2\rho^2 + \rho\right) + G_0(s)(\rho - \mu)^2\right)}{3\rho(\rho - \mu)^3} \right] \theta^3 + O(\theta^4)$$

To annihilate the second-order term, we solve

$$6\rho^4 F_0''(s) + \rho' F_0'(s)\left(\mu^2(6\rho + 1) - \mu(10\rho + 1)\rho + 4\rho^3\right) = 0$$

to get

$$F_0(s) = C_1 \int_0^s \rho^{-2/3}(t) \exp\left(\frac{2\mu^2 + 18\mu^2\rho(t) - 60\mu\rho(t)^2 - 3\mu\rho(t)}{36\rho(t)^3} \right) dt,$$

where we have fixed the additive constant so that $F_0(0) = 0$.

Solving for G_0 to annihilate the third-order term yields

$$G_0(s) = \frac{\rho^3 F_0''(s) \left(3\mu - 2\mu\rho + 2\rho^2 - \rho\right)}{(\rho - \mu)^2},$$

which with the above choice of F_0 becomes

$$G_0(s) = \frac{C_1 \left(3\mu - 2\mu\rho + 2\rho^2 - \rho\right) \left(\mu + 6\mu\rho - 4\rho^2\right) \rho' \exp\left(\frac{2\mu^2 + 18\mu^2\rho - 60\mu\rho^2 - 3\mu\rho}{36\rho^3}\right)}{6\rho^{5/3}(\rho - \mu)}.$$

Next,

$$Y_0(s, \theta) = F_0(s) - F_0(s^-) + O(\theta^2)$$

$$= F_0'(s)\theta + O(\theta^2)$$

$$= C_1 \left(\rho^{-2/3}(s) \exp\left(\frac{2\mu^2 + 18\mu^2\rho(s) - 60\mu\rho(s)^2 - 3\mu\rho(s)}{36\rho(s)^3}\right)\right)\theta + O(\theta^2).$$

To preserve the periodicity of the x-coordinate, we choose

$$C_1 = \left(\int_0^L \rho^{-2/3}(t) \exp\left(\frac{2\mu^2 + 18\mu^2\rho(t) - 60\mu\rho(t)^2 - 3\mu\rho(t)}{36\rho(t)^3}\right) dt\right)^{-1}.$$

Theorem 5. *For θ near 0 and $\mu < \rho_{min}$, consider the coordinate change given by the formulas*

$$x = X_0(s, \theta) := C_1 \int_0^s \rho^{-2/3}(t) \exp\left(\frac{2\mu^2 + 18\mu^2\rho(t) - 60\mu\rho(t)^2 - 3\mu\rho(t)}{36\rho(t)^3}\right) dt$$

$$+ \left(\frac{C_1 \left(3\mu - 2\mu\rho + 2\rho^2 - \rho\right) \left(\mu + 6\mu\rho - 4\rho^2\right) \rho' \exp\left(\frac{2\mu^2 + 18\mu^2\rho - 60\mu\rho^2 - 3\mu\rho}{36\rho^3}\right)}{6\rho^{5/3}(\rho - \mu)}\right)\theta^2 + O(\theta^4)$$

$$y = Y_0(s, \theta) := C_1 \left(\rho^{-2/3}(s) \exp\left(\frac{2\mu^2 + 18\mu^2\rho(s) - 60\mu\rho(s)^2 - 3\mu\rho(s)}{36\rho(s)^3}\right)\right)\theta + O(\theta^2),$$

where C_1 is chosen as previously stated. Then the inverse magnetic billiard map T after this coordinate change is formally conjugate to the map

$$(x, y) \mapsto (x + y, y)$$

as a power series of y. Further, these Lazutkin coordinates correspond to the Lazutkin normal form of order y^4,

$$x^+ = x + y + O(y^4) \quad \mod 1$$

$$y^+ = y + O(y^4).$$

Unfortunately we have not been able to make similar progress when T is not guaranteed to be a twist map, and so we are unable to rely upon the Lazutkin normal form construction at this time.

Of note, in the limit $\mu \to 0^+$, the x-coordinate variable change is exactly that of Lazutkin for the standard billiard map. The y-coordinate is different than that of [dSKW17], though they use a slightly different method to compute the y-coordinate than that of Lazutkin.

Repeat the above calculations near the boundary $\theta^\pm = \pi - \eta^\pm$: Consider the formal coordinate change given by assuming x and y are of the form

$$x = X_\pi(s, \eta) := F_\pi(s) + G_\pi(s)\eta^2 + O(\eta^4)$$

$$y = Y_\pi(s, \eta) := X_\pi(s, \eta) - X_\pi(s^-, \eta^-)$$

where F_π and $G\pi$ are functions to be determined. In particular, we must solve

$$K_\pi(s, \eta) := Y_\pi^+ - Y_\pi = X_\pi(s^+, \eta^+) - 2X_\pi(s, \eta) + X_\pi(s^-, \eta^-) = O(\eta^4).$$

Expand the left-hand side of this equation near $\eta = 0$ so that θ is near π. Omitting the dependence upon s, we get

$$K_\pi(s,\eta) = \left[\frac{2\left(6\rho^4 F_\pi''(s) + \rho' F_\pi'(s)\left(\mu^2(6\rho + 1) + \mu(10\rho + 1)\rho + 4\rho^3\right)\right)}{3(\rho + \mu)^2} \right] \eta^2 +$$
$$\left[\frac{4\mu\rho'\left(\rho^3 F_\pi''(s)\left(\mu(3 - 2\rho) - 2\rho^2 + \rho\right) + G_\pi(s)(\rho + \mu)^2\right)}{3\rho(\rho + \mu)^3} \right] \eta^3 + O(\eta^4)$$

To annihilate the second-order term, we solve

$$6\rho^4 F_\pi''(s) + F_\pi'(s)\left(\mu^2(6\rho + 1) + \mu(10\rho + 1)\rho + 4\rho^3\right) = 0$$

to get

$$F_\pi(s) = C_2 \int_0^s \rho^{-2/3}(t) \exp\left(\frac{2\mu^2 + 18\mu^2\rho(t) + 60\mu\rho(t)^2 + 3\mu\rho(t)}{36\rho(t)^3} \right) dt,$$

where we have fixed the additive constant so that $F_\pi(0) = 0$.

Solving for G_π to annihilate the third-order term yields

$$G_\pi(s) = \frac{\rho^3 F_\pi''(s)\left(-3\mu + (2\mu - 1)\rho + 2\rho^2\right)}{(\rho + \mu)^2},$$

which with the above choice of F_π becomes

$$G_\pi(s) = \frac{C_2\left(3\mu - (2\mu - 1)\rho - 2\rho^2\right)\left(\mu + 6\mu\rho + 4\rho^2\right)\rho' \exp\left(\frac{2\mu^2 + 18\mu^2\rho + 60\mu\rho^2 + 3\mu\rho}{36\rho^3} \right)}{6\rho^{5/3}(\rho + \mu)}.$$

Next,

$$Y_\pi(s,\eta) = F_\pi(s) - F_\pi(s^-) + O(\eta^2)$$
$$= F_\pi'(s)\eta + O(\eta^2)$$

$$= C_2 \left(\rho^{-2/3}(s) \exp \left(\frac{2\mu^2 + 18\mu^2\rho(s) + 60\mu\rho(s)^2 + 3\mu\rho(s)}{36\rho(s)^3} \right) \right) \eta + O(\eta^2).$$

To preserve the periodicity of the x-coordinate, we choose

$$C_2 = \left(\int_0^L \rho^{-2/3}(t) \exp \left(\frac{2\mu^2 + 18\mu^2\rho(t) + 60\mu\rho(t)^2 + 3\mu\rho(t)}{36\rho(t)^3} \right) dt \right)^{-1}.$$

Theorem 6. *For $\theta = \pi - \eta$ with η near 0 and $\mu < \rho_{min}$, consider the coordinate change given by the formulas*

$$x = X_\pi(s, \eta) := C_2 \int_0^s \rho^{-2/3}(t) \exp \left(\frac{2\mu^2 + 18\mu^2\rho(t) + 60\mu\rho(t)^2 + 3\mu\rho(t)}{36\rho(t)^3} \right) dt$$

$$+ \left(\frac{C_2 \left(3\mu - (2\mu - 1)\rho - 2\rho^2\right)\left(\mu + 6\mu\rho + 4\rho^2\right)\rho' \exp \left(\frac{2\mu^2+18\mu^2\rho+60\mu\rho^2+3\mu\rho}{36\rho^3} \right)}{6\rho^{5/3}(\rho + \mu)} \right) \eta^2 + O(\eta^4)$$

$$y = Y_\pi(s, \eta) := C_2 \left(\rho^{-2/3}(s) \exp \left(\frac{2\mu^2 + 18\mu^2\rho(s) + 60\mu\rho(s)^2 + 3\mu\rho(s)}{36\rho(s)^3} \right) \right) \eta + O(\eta^2),$$

where C_2 is chosen as previously stated. Then the inverse magnetic billiard map T after this coordinate change is formally conjugate to the map

$$(x, y) \mapsto (x + y, y)$$

as a power series of y. Further, these Lazutkin coordinates correspond to the Lazutkin normal form of order y^4,

$$x^+ = x + y + O(y^4) \mod 1$$
$$y^+ = y + O(y^4).$$

Unlike the previous theorem, this coordinate change is defined for all values

46

of μ as the denominators never vanish, and so we may expect invariant curves for all values of μ when θ is near π. This is consistent with our results of the previous section. In the limit $\mu \to 0^+$, the first coordinate change approaches that of Lazutkin.

From the previous two theorems, we may apply the Lazutkin and KAM theorems to imply the existence of invariant curves in the cases when $\mu < \rho_{min}$ and $\theta \approx 0$ or $\theta \approx \pi$, with a sufficiently smooth boundary. This is consistent with our results from Section 3.2 using a different technique. However, what is not immediately known is if the caustics guaranteed by the theorems from Sections 3.2 and 3.3 are the same.

In the case of standard billiards, Lazutkin's work shows there is an intricate connection between caustics and a particular geometric quantity called the *Lazutkin parameter* defined as follows:

Definition 8 ([Ami97]). *For a simple and strictly convex curve $C \subset \Omega$ and a point $P \in \partial\Omega$, there are exactly two points $a, b \in C$ so that the tangent lines to C at a and b go through P. We assume that b follows a according to a fixed orientation of C. Denote the lengths of the line segments between a and P and between b and P by l and m. Further, let the arc length along C from a and b (induced by the orientation of C) be denoted by n. Then the **Lazutkin parameter** Q of C and Ω at P is*

$$Q(C, \partial\Omega, P) = l + m - n.$$

Proposition 11 ([Laz73], [Ami97]). *In standard billiards, a strictly convex simple closed planar curve $C \subset \Omega$ is a caustic if and only if the Lazutkin parameter of C and $\partial\Omega$ at $P \in \partial\Omega$ is independent of the point P. In fact, if s denotes the arc length along $\partial\Omega$,*

$$\frac{d}{ds}Q(C, \partial\Omega, P) = \cos(\theta^+) - \cos(\theta^-)$$

where $\theta^\pm$ are the angles made by the tangent to $\partial\Omega$ at P with the forward and backward rays from C to P (in the notation above, the forward ray is the one from a to P).

What is unknown at the moment is the analogous version of a Lazutkin parameter for inverse magnetic billiards and inner caustics.

Chapter 4

Conclusions and Next Steps

We have found that inverse magnetic billiards shares some similarities with standard and magnetic billiards while also showing concrete differences. The influence of the magnetic field on the dynamics is significant, and we have clearly seen that inverse magnetic billiards is a nontrivial perturbation of the standard billiard.

The behavior of inverse magnetic billiards in the regimes $\rho_{min} < \mu < \rho_{max}$ and $\rho_{max} < \mu$ are not well understood at this time. For example, numerical simulations seem to show the existence of a C^0 caustic comprised of piecewise C^1 curves. See Figure 4.1. Of further interest is the locus of the centers of the Larmor circles in such a case, as these centers appear to lie on a smooth simple closed curve with two axes of symmetry. Further, it seems that understanding properties of the map which sends the center of one Larmor circle to the next would be of interest. What are its properties? Does it preserve any measure? Are there any dynamics associated to this map?

Another aspect of inverse magnetic billiards that has not been studied is the existence of *outer* caustics. Figures 2.6, 3.3, 4.1 all show the existence of exterior caustics, and this phenomena is certainly worth investigating.
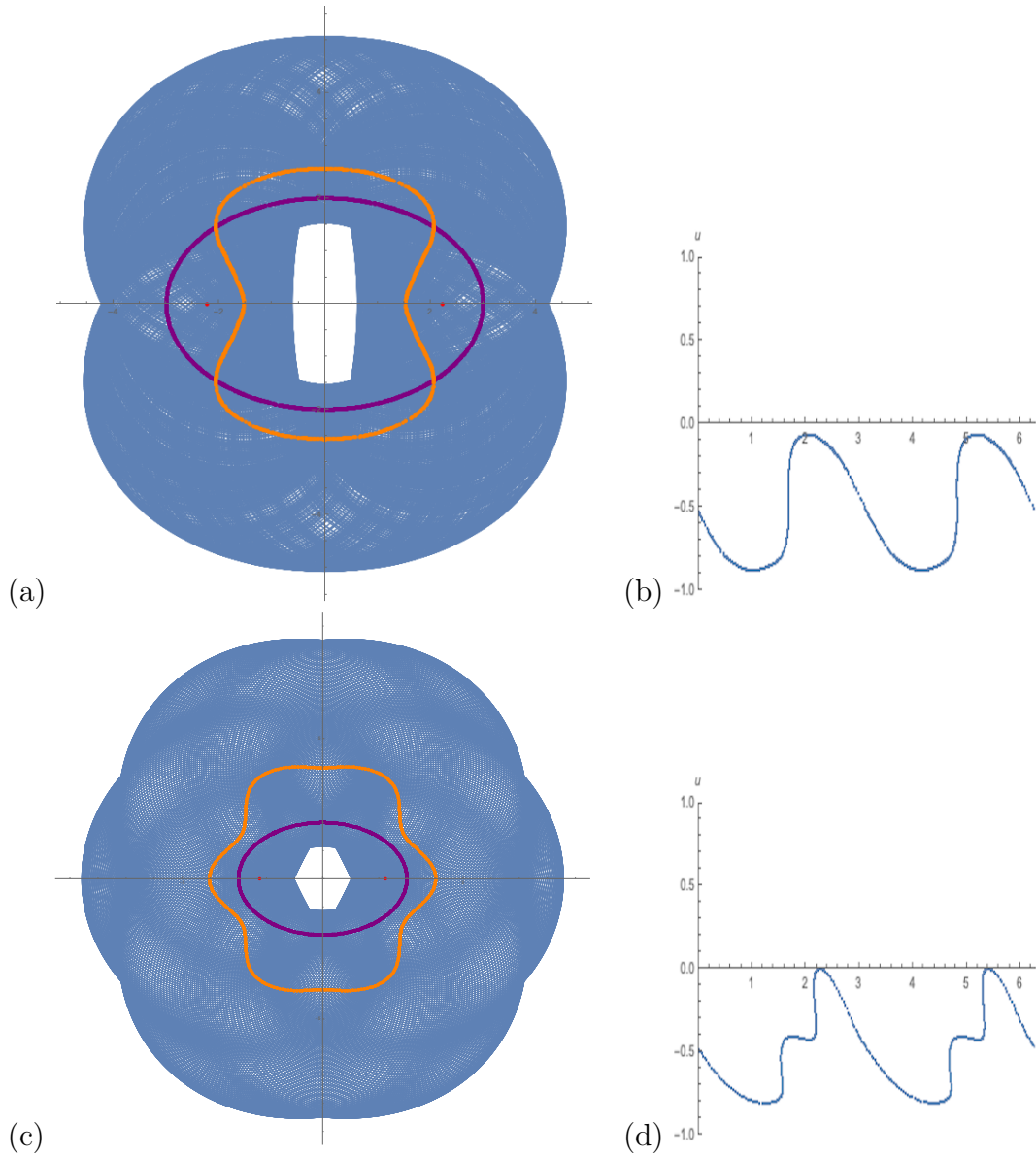
Figure 4.1: C^0 caustics in an ellipse for the two non-twist curvature regimes and 10^3 iterations of T: (a) $\rho_{min} < \mu < \rho_{max}$; (c) $\rho_{max} < \mu$; and their accompanying invariant curves in the (ϕ, u)-plane, (b), (d), respectively. The centers of the Larmor circles are marked in orange, the foci of the ellipse are in red, and the points P_i are in dark purple.

Further changes can be made to this setting that have not been explored. If the magnetic field has a piecewise constant strength outside of Ω, the Larmor arcs of two fixed radii are concatenated before returning, or potentially not returning, to Ω. Investigating this scenario is the next step towards understanding a completely variable magnetic field outside Ω. In addition, the presence of an electric field (or an arbitrary potential) would influence the dynamics in a concrete way. This was done briefly in [Ber96] for exterior magnetic billiards outside a circle by introducing an electric field and treating the problem as a scattering system.

Appendix A

Detailed Proofs of Certain

Theorems and Propositions

A.1   Proof of Proposition 1

Construct a local coordinate system with P_1 at the origin with the outgoing velocity of the trajectory at P_1 in the positive horizontal direction. Replace $\Gamma(s)$ with its osculating circle at P_1, $\mathcal{O}_\Gamma(s_1)$ with radius ρ_1. The center of the Larmor circle is $G = (0, \mu)$ and the center of $\mathcal{O}_\Gamma(s_1)$ is $F = (-\rho_1 \sin(\theta_1), \rho_1 \cos(\theta_1))$. Further, define $\beta = \angle P_1 F G$ and let $z = |FG|$. Approximate the reentry point P_2 by the intersection point between the Larmor circle and $\mathcal{O}_\Gamma(s_1)$ other than P_1, P_2^*, so that we approximate χ by χ^*, the angle between the horizontal axis and the chord $P_1 P_2^*$.

Through simple Euclidean geometry, we get

$$\chi^* = \theta_1 + \beta$$

$$\ell_2 \approx \frac{1}{z}\sqrt{4z^2\rho_1^2 - (z^2 - \mu^2 + \rho_1^2)^2} = \frac{2\mu\rho_1 \sin(\theta_1)}{z}$$
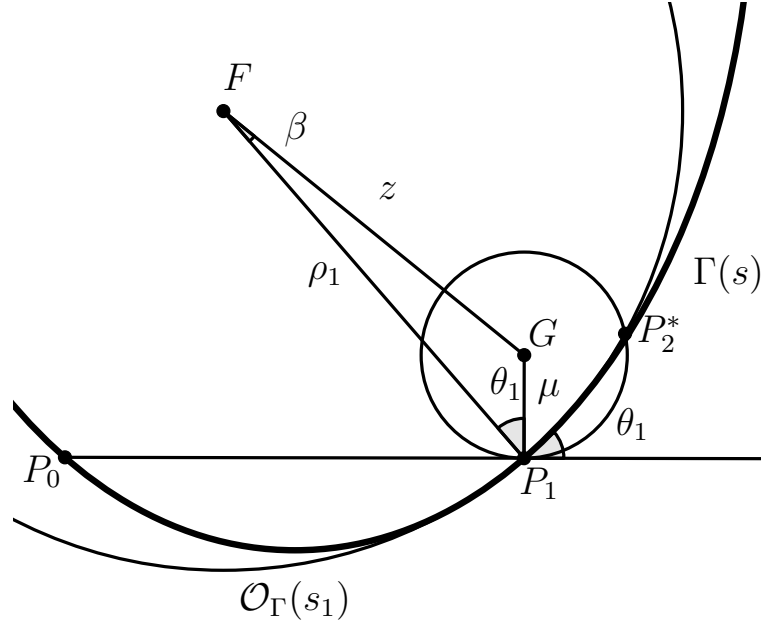
Figure A.1: A labeled diagram to approximate χ when $\mu < \rho_{min}$. A similar diagram holds for the other curvature regimes.

where

$$
\beta = \begin{cases} \arcsin\left(\frac{\mu\sin(\theta_1)}{z}\right) \\ \pi - \arcsin\left(\frac{\mu\sin(\theta_1)}{z}\right) \end{cases}
$$

depending upon whether β, as shown in Figure A.1 is less than or greater than $\frac{\pi}{2}$, respectively, to accommodate for the range of the inverse sine function. We note that when Γ is a circle, these equations are exact.

We can compute $z = \sqrt{\mu^2 + \rho_1^2 - 2\mu\rho_1\cos(\theta_1)}$ using the law of cosines, but it will be useful to us to make several simplifying assumptions. Suppose θ_1 is sufficiently small. Observe that when $\mu < \rho_{min}$, $z \approx \rho_1 - \mu$, and when $\rho_{max} < \mu$, $z \approx \mu - \rho_1 = -(\rho_1 - \mu)$. This means that

$$
\chi^*(\theta_1) \approx \begin{cases} \theta_1 + \arcsin\left(\frac{\mu\sin(\theta_1)}{\rho_1-\mu}\right) & \text{if } \mu < \rho_{min} \\ \theta_1 + \pi - \arcsin\left(\frac{\mu\sin(\theta_1)}{-(\rho_1-\mu)}\right) & \text{if } \rho_{max} < \mu. \end{cases}
$$

Importantly, the denominators of both expressions above are guaranteed to be nonzero.

Expanding this approximation as a series for θ_1,

$$
\chi \approx \chi^*(\theta_1) \approx
\begin{cases}
\frac{\rho_1}{\rho_1 - \mu}\theta_1 + O(\theta_1^3) = \frac{1}{1-\mu\kappa_1}\theta_1 + O(\theta_1^3) & \text{if } \mu < \rho_{min} \\
\pi + \frac{\rho_1}{\rho_1 - \mu}\theta_1 + O(\theta_1^3) = \pi + \frac{1}{1-\mu\kappa_1}\theta_1 + O(\theta_1^3) & \text{if } \rho_{max} < \mu,
\end{cases}
$$

which ultimately means

$$
\frac{\partial\chi}{\partial\theta_1} \approx \frac{\rho_1}{\rho_1 - \mu} + O(\theta_1^2)
$$

in both of the two aforementioned curvature regimes.

When $\theta_1 = \pi - \eta_1$, the approximations

$$
\chi(\eta_1) \approx \pi - \eta_1 + \arcsin\left(\frac{\mu \sin(\eta_1)}{\rho_1 + \mu}\right)
$$

and

$$
\frac{\partial\chi}{\partial\eta_1} \approx -\frac{\rho_1}{\rho_1 + \mu} + O(\eta_1^2)
$$

follow from an identical approach.

A.2 Proof of Proposition 2

Consider the line segment trajectory portion of Figure 2.1. For the sake of notation, write $X_i = X(s_i)$ and $Y_i = Y(s_i)$. Define

$$
\alpha_0 = \arg[(X_1 - X_0) + i(Y_1 - Y_0)],
$$

the polar angle between the positive x-axis and the segment $P_0 P_1$, and let $\tau_i = \tau(s_i)$ for $i = 0, 1, 2$. And in a slight abuse of notation,

$$\frac{\partial \tau_i}{\partial s_i} = \kappa(s_i) =: \kappa_i, \quad i = 0, 1, 2.$$

by the definition of curvature. See Figure A.2. By construction we see that

$$\theta_0 = \alpha_0 - \tau_0 \quad \text{and} \quad \theta_1 = \tau_1 - \alpha_0.$$
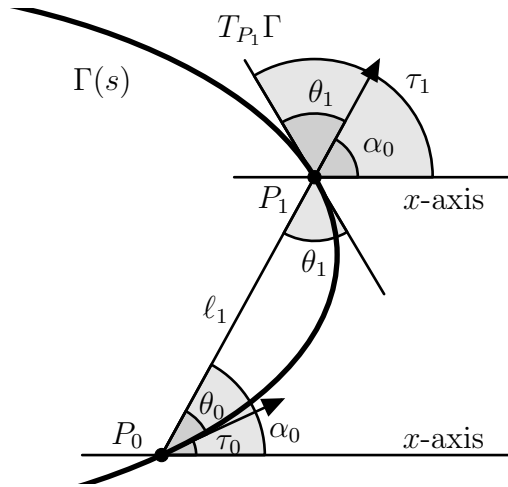
Figure A.2: A labeled picture of the $P_0 P_1$ portion of a trajectory.

From our construction, we also see that

$$\ell_1^2 = (X_1 - X_0)^2 + (Y_1 - Y_0)^2. \tag{A.2.1}$$

From (A.2.1) we determine the following:

$$\tan(\alpha_0) = \frac{Y_1 - Y_0}{X_1 - X_0}$$

$$\frac{\partial \alpha_0}{\partial s_0} = \frac{1}{\ell_1^2} \left[(Y_1 - Y_0)X'(s_0) - (X_1 - X_0)Y'(s_0) \right]$$

$$= \frac{1}{\ell_1^2} \left[\ell_1 \sin(\alpha_0) \cos(\tau_0) - \ell_1 \cos(\alpha_0) \sin(\tau_0) \right] = \frac{\sin(\theta_0)}{\ell_1}.$$

Since $\theta_0 = \alpha_0 - \tau_0$ and $\theta_1 = \tau_1 - \alpha_0$, differentiate both sides with respect to s_0 to get

$$\frac{\partial \theta_0}{\partial s_0} = \frac{\sin(\theta_0)}{\ell_1} - \kappa_0$$

$$\frac{\partial \theta_1}{\partial s_0} = -\frac{\sin(\theta_0)}{\ell_1}.$$

Repeating the above argument but with respect to s_1 yields

$$\frac{\partial \alpha_0}{\partial s_1} = \frac{\sin(\theta_1)}{\ell_1}$$

$$\frac{\partial \theta_0}{\partial s_1} = \frac{\sin(\theta_1)}{\ell_1}$$

$$\frac{\partial \theta_1}{\partial s_1} = \kappa_1 - \frac{\sin(\theta_1)}{\ell_1}.$$

We now want to solve the following linear system for ds_1 and $d\theta_1$ in terms of ds_0 and $d\theta_0$:

$$d\theta_0 = \frac{\partial \theta_0}{\partial s_0} ds_0 + \frac{\partial \theta_0}{\partial s_1} ds_1$$

$$d\theta_1 = \frac{\partial \theta_1}{\partial s_0} ds_0 + \frac{\partial \theta_1}{\partial s_1} ds_1$$

and get

$$ds_1 = \left(-\frac{\frac{\partial \theta_0}{\partial s_0}}{\frac{\partial \theta_0}{\partial s_1}} \right) ds_0 + \left(\frac{1}{\frac{\partial \theta_0}{\partial s_1}} \right) d\theta_0$$

$$d\theta_1 = \left(\frac{\frac{\partial \theta_1}{\partial s_0} \frac{\partial \theta_0}{\partial s_1} - \frac{\partial \theta_1}{\partial s_1} \frac{\partial \theta_0}{\partial s_0}}{\frac{\partial \theta_0}{\partial s_1}} \right) ds_0 + \left(\frac{\frac{\partial \theta_1}{\partial s_1}}{\frac{\partial \theta_0}{\partial s_1}} \right) d\theta_0.$$

Recall that $u_i = -\cos(\theta_i)$, so that $du_i = \sin(\theta_i)d\theta_i$ for each i. Adjusting the above equations to be in terms of ds_1 and du_1, we get

$$ds_1 = \left(-\frac{\frac{\partial \theta_0}{\partial s_0}}{\frac{\partial \theta_0}{\partial s_1}} \right) ds_0 + \left(\frac{1}{\sin(\theta_0)\frac{\partial \theta_0}{\partial s_1}} \right) du_0$$

$$du_1 = \sin(\theta_1) \left(\frac{\frac{\partial \theta_1}{\partial s_0}\frac{\partial \theta_0}{\partial s_1} - \frac{\partial \theta_1}{\partial s_1}\frac{\partial \theta_0}{\partial s_0}}{\frac{\partial \theta_0}{\partial s_1}} \right) ds_0 + \frac{\sin(\theta_1)}{\sin(\theta_0)} \left(\frac{\frac{\partial \theta_1}{\partial s_1}}{\frac{\partial \theta_0}{\partial s_1}} \right) du_0.$$

This tells us ultimately that

$$\frac{\partial s_1}{\partial s_0} = -\frac{\frac{\partial \theta_0}{\partial s_0}}{\frac{\partial \theta_0}{\partial s_1}}$$

$$\frac{\partial s_1}{\partial u_0} = \frac{1}{\sin(\theta_0)\frac{\partial \theta_0}{\partial s_1}}$$

$$\frac{\partial u_1}{\partial s_0} = \sin(\theta_1) \left(\frac{\frac{\partial \theta_1}{\partial s_0}\frac{\partial \theta_0}{\partial s_1} - \frac{\partial \theta_1}{\partial s_1}\frac{\partial \theta_0}{\partial s_0}}{\frac{\partial \theta_0}{\partial s_1}} \right)$$

$$\frac{\partial u_1}{\partial u_0} = \frac{\sin(\theta_1)}{\sin(\theta_0)} \left(\frac{\frac{\partial \theta_1}{\partial s_1}}{\frac{\partial \theta_0}{\partial s_1}} \right).$$

Computing each of these factors using the equations we have previously derived produces

$$\frac{\partial s_1}{\partial s_0} = \frac{\kappa_0 \ell_1 - \sin(\theta_0)}{\sin(\theta_1)}$$

$$\frac{\partial s_1}{\partial u_0} = \frac{\ell_1}{\sin(\theta_0)\sin(\theta_1)}$$

$$\frac{\partial u_1}{\partial s_0} = \kappa_0 \kappa_1 \ell_1 - \kappa_1 \sin(\theta_0) - \kappa_0 \sin(\theta_1)$$

$$\frac{\partial u_1}{\partial u_0} = \frac{\kappa_1 \ell_1 - \sin(\theta_1)}{\sin(\theta_0)}.$$

This completes the proof of the components of DT_1.

Next, consider a single magnetic arc, as in Figure 2.2a. We will mimic the

57

previous series of calculations. As before, define

$$\alpha_1 = \arg[(X_2 - X_1) + i(Y_2 - Y_1)],$$

the polar angle between the positive x-axis and the segment $P_1 P_2$. Figure A.3 demonstrates that $\tau_1 - \theta_1 = \alpha_1 - \chi$. A similar picture centered on P_2 tells us that $\tau_2 = \alpha_1 + \chi - \theta_2$. This leads to the following equations:

$$\theta_1 = \tau_1 - \alpha_1 + \chi$$

$$\theta_2 = \alpha_1 + \chi - \tau_2.$$
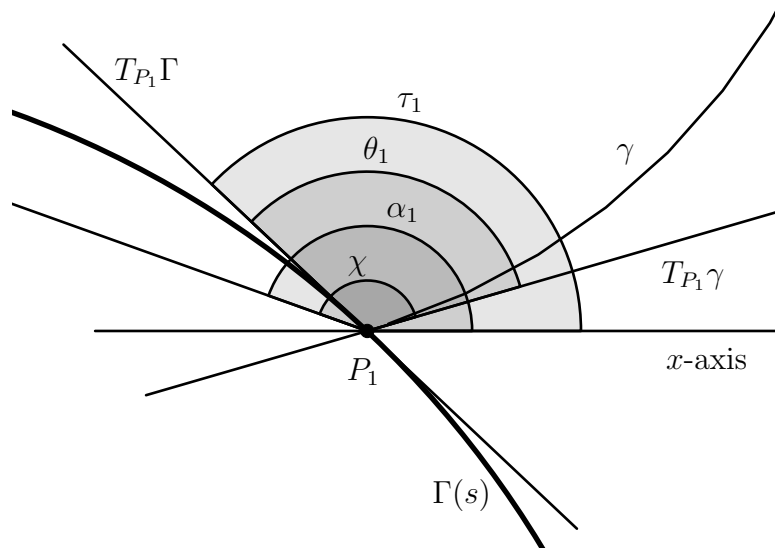
Figure A.3: A labeled picture close to P_1 on $\Gamma(s)$.

By construction, we also see that

$$\ell_2^2 = (X_2 - X_1)^2 + (Y_2 - Y_1)^2. \tag{A.2.2}$$

58

From (A.2.2) we determine the following:

$$\tan(\alpha_1) = \frac{Y_2 - Y_1}{X_2 - X_1}$$

$$\frac{\partial \alpha_1}{\partial s_1} = \frac{1}{\ell_2^2} [(Y_2 - Y_1)X'(s_1) - (X_2 - X_1)Y'(s_1)]$$

$$= \frac{1}{\ell_2^2} [\ell_2 \sin(\alpha_1) \cos(\tau_1) - \ell_2 \cos(\alpha_1) \sin(\tau_1)] = \frac{\sin(\chi - \theta_1)}{\ell_2}.$$

Differentiating (A.2.2) with respect to s_1 yields

$$\frac{\partial \ell_2}{\partial s_1} = \frac{1}{2\ell_2} [2(X_2 - X_1)(-X'(s_1)) + 2(Y_2 - Y_1)(-Y'(s_1))]$$

$$= -[\cos(\tau_1) \cos(\alpha_1) + \sin(\tau_1) \sin(\alpha_1)]$$

$$= -\cos(\theta_1 - \chi).$$

Next, differentiate $\sin(\chi) = \frac{\ell_2}{2\mu}$ with respect to s_1 and solve for $\frac{\partial \chi}{\partial s_1}$ to get

$$\frac{\partial \chi}{\partial s_1} = \frac{1}{\ell_2 \cos(\chi)} \frac{\ell_2}{2\mu} \frac{\partial \ell_2}{\partial s_1}$$

$$= -\frac{\sin(\chi) \cos(\theta_1 - \chi)}{\ell_2 \cos(\chi)}.$$

Next, we differentiate the angle formulas for θ_1, θ_2 with respect to s_1 to get

$$\frac{\partial \theta_1}{\partial s_1} = \frac{\partial \tau_1}{\partial s_1} - \frac{\partial \alpha_1}{\partial s_1} + \frac{\partial \chi}{\partial s_1} = \kappa_1 - \frac{\sin(2\chi - \theta_1)}{\ell_2 \cos(\chi)}$$

$$\frac{\partial \theta_2}{\partial s_1} = \frac{\partial \alpha_1}{\partial s_1} + \frac{\partial \chi}{\partial s_1} - \frac{\partial \tau_2}{\partial s_1} = -\frac{\sin(\theta_1)}{\ell_2 \cos(\chi)}.$$

Repeating this process again but with respect to s_2 yields the following:

$$\frac{\partial \alpha_1}{\partial s_2} = \frac{\sin(\chi - \theta_2)}{\ell_2}$$

$$\frac{\partial \tau_2}{\partial s_2} = \kappa(s_2) =: \kappa_2$$

59

$$\frac{\partial \ell_2}{\partial s_2} = \cos(\chi - \theta_2)$$

$$\frac{\partial \chi}{\partial s_2} = \frac{\sin(\chi)\cos(\chi - \theta_2)}{\ell_2 \cos(\chi)}.$$

Differentiate the angle formulas for θ_1, θ_2 with respect to s_2 and simplify to get

$$\frac{\partial \theta_1}{\partial s_2} = \frac{\sin(\theta_2)}{\ell_2 \cos(\chi)}$$

$$\frac{\partial \theta_2}{\partial s_2} = \frac{\sin(2\chi - \theta_2)}{\ell_2 \cos(\chi)} - \kappa_2.$$

We now want to solve the following linear system for ds_2 and $d\theta_2$ in terms of ds_1 and $d\theta_1$:

$$d\theta_1 = \frac{\partial \theta_1}{\partial s_1} ds_1 + \frac{\partial \theta_1}{\partial s_2} ds_2$$

$$d\theta_2 = \frac{\partial \theta_2}{\partial s_1} ds_1 + \frac{\partial \theta_2}{\partial s_2} ds_2$$

and get

$$ds_2 = \left(-\frac{\frac{\partial \theta_1}{\partial s_1}}{\frac{\partial \theta_1}{\partial s_2}} \right) ds_1 + \left(\frac{1}{\frac{\partial \theta_1}{\partial s_2}} \right) d\theta_1$$

$$d\theta_2 = \left(\frac{\frac{\partial \theta_2}{\partial s_1}\frac{\partial \theta_1}{\partial s_2} - \frac{\partial \theta_2}{\partial s_2}\frac{\partial \theta_1}{\partial s_1}}{\frac{\partial \theta_1}{\partial s_2}} \right) ds_1 + \left(\frac{\frac{\partial \theta_2}{\partial s_2}}{\frac{\partial \theta_1}{\partial s_2}} \right) d\theta_1.$$

Recall that $u_i = -\cos(\theta_i)$, so that $du_i = \sin(\theta_i)d\theta_i$ for each i. Adjusting the above equations to be in terms of ds_2 and du_2, we get

$$ds_2 = \left(-\frac{\frac{\partial \theta_1}{\partial s_1}}{\frac{\partial \theta_1}{\partial s_2}} \right) ds_1 + \left(\frac{1}{\sin(\theta_1)\frac{\partial \theta_1}{\partial s_2}} \right) du_1$$

60

$$du_2 = \sin(\theta_2) \left(\frac{\frac{\partial \theta_2}{\partial s_1} \frac{\partial \theta_1}{\partial s_2} - \frac{\partial \theta_2}{\partial s_2} \frac{\partial \theta_1}{\partial s_1}}{\frac{\partial \theta_1}{\partial s_2}} \right) ds_1 + \frac{\sin(\theta_2)}{\sin(\theta_1)} \left(\frac{\frac{\partial \theta_2}{\partial s_2}}{\frac{\partial \theta_1}{\partial s_2}} \right) du_1.$$

This tells us ultimately that

$$\frac{\partial s_2}{\partial s_1} = -\frac{\frac{\partial \theta_1}{\partial s_1}}{\frac{\partial \theta_1}{\partial s_2}}$$

$$\frac{\partial s_2}{\partial u_1} = \frac{1}{\sin(\theta_1)\frac{\partial \theta_1}{\partial s_2}}$$

$$\frac{\partial u_2}{\partial s_1} = \sin(\theta_2) \left(\frac{\frac{\partial \theta_2}{\partial s_1} \frac{\partial \theta_1}{\partial s_2} - \frac{\partial \theta_2}{\partial s_2} \frac{\partial \theta_1}{\partial s_1}}{\frac{\partial \theta_1}{\partial s_2}} \right)$$

$$\frac{\partial u_2}{\partial u_1} = \frac{\sin(\theta_2)}{\sin(\theta_1)} \left(\frac{\frac{\partial \theta_2}{\partial s_2}}{\frac{\partial \theta_1}{\partial s_2}} \right).$$

Computing each of these factors using the equations we have previously derived produces

$$\frac{\partial s_2}{\partial s_1} = \frac{\sin(2\chi - \theta_1) - \ell_2\kappa_1 \cos(\chi)}{\sin(\theta_2)}$$

$$\frac{\partial s_2}{\partial u_1} = \frac{\ell_2 \cos(\chi)}{\sin(\theta_1)\sin(\theta_2)}$$

$$\frac{\partial u_2}{\partial s_1} = \frac{\sin(2\chi - \theta_1)\sin(2\chi - \theta_2) - \sin(\theta_1)\sin(\theta_2)}{\ell_2 \cos(\chi)}$$

$$- \kappa_1 \sin(2\chi - \theta_2) - \kappa_2 \sin(2\chi - \theta_1) + \kappa_1\kappa_2\ell_2 \cos(\chi)$$

$$\frac{\partial u_2}{\partial u_1} = \frac{\sin(2\chi - \theta_2) - \kappa_2\ell_2 \cos(\chi)}{\sin(\theta_1)}.$$

This completes the proof of the components of DT_2. We also note the similarity of these terms to those occurring in Proposition 1 of [BK96], as we would expect.

A.3 Proof of Proposition 3

We wish to show that if $\mu < \rho_{min}$, then

$$\ell_1 \sin(2\chi - \theta_1) - \ell_2 \cos(\chi) \sin(\theta_1) > 0.$$

Instead we will show an equivalent statement which follows from the equation $\ell_2 \cos(\chi) = \mu \sin(2\chi)$ and the positivity of $\sin(\theta_1)$:

$$\frac{\sin(2\chi - \theta_1)}{\sin(\theta_1)}\ell_1 - \mu \sin(2\chi) > 0. \tag{A.3.1}$$

First, since $\mu < \rho_{min}$, we use that the approximation

$$\chi \approx \chi^*(\theta_1) = \theta_1 + \arcsin\left(\frac{\mu \sin(\theta_1)}{\sqrt{\mu^2 + \rho_1^2 - 2\mu\rho_1 \cos(\theta_1)}}\right),$$

which does well near $\theta_1 = 0$ and π. The convexity of $\partial\Omega$ implies that χ is almost always increasing (with some occasional exceptions near points of extreme curvature). Since $0 < \theta_1 < \chi$ by construction, we have that $2\chi - \theta_1 > 0$. Further, as $\theta_1 \to \pi^-$, we see that $\chi \to \pi^-$ as well, which in turns implies that $2\chi - \theta_1 < \pi$ for all $0 < \theta_1 < \pi$. Because $\ell_1 > 0$, we observe that

$$\frac{\sin(2\chi - \theta_1)}{\sin(\theta_1)}\ell_1 > 0$$

for all θ_1, χ under consideration. Furthermore, this implies that (A.3.1) is satisfied if $\frac{\pi}{2} \leq \chi < \pi$.

Assume that $0 < \chi < \frac{\pi}{2}$. Using the geometry of a circle, we can also see that

$\ell_1 \geq 2\rho_{min} \sin(\theta_1)$. Then

$$\frac{\sin(2\chi - \theta_1)}{\sin(\theta_1)} \ell_1 - \mu \sin(2\chi) \geq 2\rho_{min} \sin(2\chi - \theta_1) - \mu \sin(2\chi) > 0$$

if and only if

$$\frac{2\sin(2\chi - \theta_1)}{\sin(2\chi)} > \frac{\mu}{\rho_{min}}. \qquad (A.3.2)$$

However, because the right side of (A.3.2) is less than 1 by assumption, it is sufficient to show that the left side of (A.3.2) is greater than or equal to 1. Observe that

$$\begin{aligned}
\frac{2\sin(2\chi - \theta_1)}{\sin(2\chi)} &= \frac{2\sin(\chi + \chi - \theta_1)}{\sin(2\chi)} \\
&= \frac{2(\sin(\chi)\cos(\chi - \theta_1) + \sin(\chi - \theta_1)\cos(\chi))}{2\sin(\chi)\cos(\chi)} \\
&= \frac{\cos(\chi - \theta_1)}{\cos(\chi)} + \frac{\sin(\chi - \theta_1)}{\sin(\chi)} \\
&> 1
\end{aligned}$$

because the sine and cosine functions are increasing and decreasing on the interval $(0, \frac{\pi}{2})$, respectively. Because

$$\frac{2\sin(2\chi - \theta_1)}{\sin(2\chi)} > 1 > \frac{\mu}{\rho_{min}},$$

this implies that (A.3.1) is satisfied whenever $\mu < \rho_{min}$.

A.4   Proof of a Geometric Proposition

The following proposition is no longer needed, but we include it in case it could be of some use in the future.

Proposition 12. *If $\mu < \rho_{min}$, then $\ell_1 + \ell_2 \cos(\chi) > 0$.*

This proof is lengthy and technical, though the only tools necessary are a bit of plane geometry and some ingenuity. We begin with a few observations. The first is that

$$\ell_1 + \ell_2 \cos(\chi) > 0 \iff \ell_1^2 + \ell_1 \ell_2 \cos(\chi) > 0$$
$$\iff \overrightarrow{P_0 P_1} \cdot \overrightarrow{P_0 P_1} + \overrightarrow{P_0 P_1} \cdot \overrightarrow{P_1 P_2} > 0$$
$$\iff \overrightarrow{P_0 P_1} \cdot (\overrightarrow{P_0 P_1} + \overrightarrow{P_1 P_2}) > 0$$
$$\iff \overrightarrow{P_0 P_1} \cdot \overrightarrow{P_0 P_2} > 0.$$
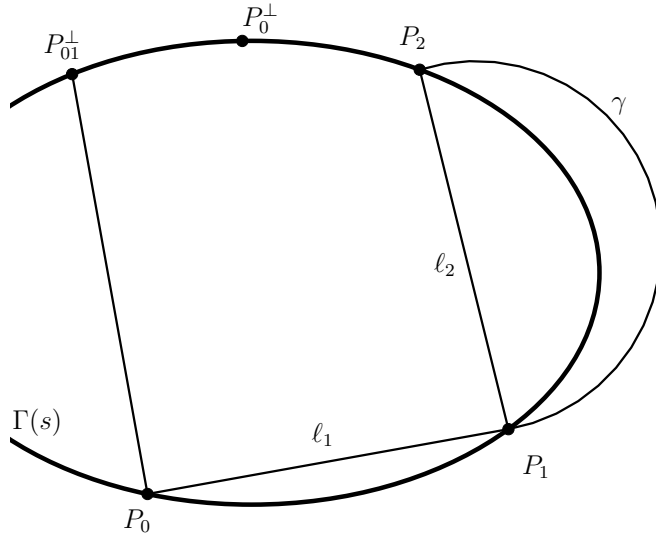
Figure A.4: Labeling the relative positions of P_0, P_1, P_2 and $P_{01}^\perp$.

Construct the perpendicular line to $P_0 P_1$ through P_0 and let $P_{01}^\perp$ be the other point of intersection of this line with $\Gamma(s)$ (other that P_0, that is). Furthermore, construct the normal line to $\Gamma(s)$ at P_0 and denote the other point of intersection as $P_0^\perp$. To keep the above dot product positive we simply need P_2 to be on the same side of line $\overleftrightarrow{P_0 P_{01}^\perp}$ as P_1. See Figure A.4.

64

Another observation is that when $\theta_0 = \frac{\pi}{2}$, $P_1 = P_0^\perp$ and $P_{01}^\perp = P_0$, which in turn implies that the dot product condition is satisfied. From this we see that when $\theta_0 > \frac{\pi}{2}$, the circular arc is on the opposite side of line $P_0 P_1$ from the point $P_{01}^\perp$ (as the points appearing in "counterclockwise" order would be P_0, $P_{01}^\perp$, $P_0^\perp$, P_1, P_2) for any positive value of μ. This implies that the return map T is a twist map $\ell_1 + \ell_2 \cos(\chi) > 0$ whenever $\theta_0 > \frac{\pi}{2}$. See Figure A.5.

Lemma 2. *When $\mu > \rho_{min}$, the expression $\ell_1 + \ell_2 \cos(\chi)$ is not necessarily strictly positive or strictly negative for all initial conditions (s_0, θ_0).*

Proof. We merely observe two statements made in the prior paragraphs. If $\theta_0 > \frac{\pi}{2}$, P_2 is on the same side of $\overleftrightarrow{P_0 P_{01}^\perp}$ as P_1. But when $0 < \theta_0 < \frac{\pi}{2}$ and μ is sufficiently large, P_2 will lie on the opposite side of $\overleftrightarrow{P_0 P_{01}^\perp}$ as P_1. This will make $\ell_1 + \ell_2 \cos(\chi)$ have opposite signs for certain values of θ_0. $\square$
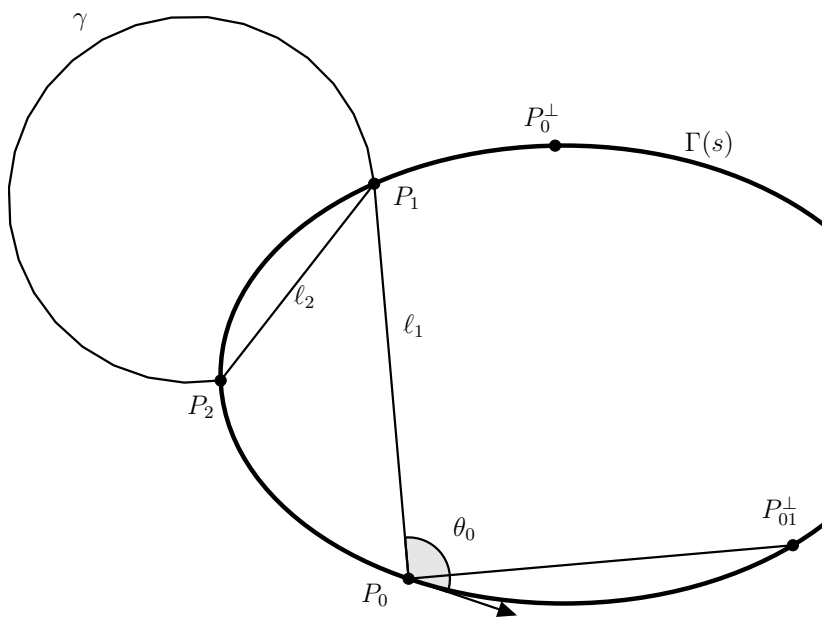
Figure A.5: The case when $\theta_0 > \frac{\pi}{2}$ implying $\ell_1 + \ell_2 \cos(\chi) > 0$ using the equivalent dot product condition.

With the above observation, we see that if we can show that $\ell_1 + \ell_2 \cos(\chi) > 0$ for $0 < \theta_0 < \frac{\pi}{2}$, we will be showing that $\ell_1 + \ell_2 \cos(\chi) > 0$ for all admissible values of θ_0.

To that end, we turn to a classical "rolling ball" theorem by Blaschke in 1916.

Theorem 7 ([Bla16]). *Assume that the convex domain $\Omega \subset \mathbb{R}^2$ has C^2 boundary $\Gamma = \partial\Omega$ and that with the positive constant $\kappa' > 0$ the curvature satisfies $\kappa(z) \leq \kappa'$ at all boundary points $z \in \Gamma$. Then to each boundary point $z \in \Gamma$ there exists a disk D_R of radius $R = 1/\kappa'$ such that $z \in \partial D_R$ and $D_R \subset \Omega$.*

An interpretation of this theorem is that provided Ω is a convex set and Γ is C^2, a ball of radius less than or equal to $R = 1/\kappa'$ can smoothly roll along Γ on the interior of Ω without slipping. This will be useful in due time.

Next, we prove a few statements about intersection points of a pair of circles:

Lemma 3. *Consider the following picture. The circle C_R has center A and radius R and the circle C_r has center F and radius r. Let CD be a chord of circle C_R with midpoint I and with circle C_r tangent to chord CD at D. Furthermore, let points E and G be the endpoints of the unique diameter of C_R that is perpendicular to CD. And let H be the point of intersection between C_R and C_r other than D. Then the following are true:*

1. *There exists a unique circle $\mathcal{C}$ tangent to CD at D that goes through D and G. This circle $\mathcal{C}$ has radius $\frac{|ID|^2 + |IG|^2}{2|IG|}$.*

2. *$G = H$ if and only if $r = R$. Furthermore, if $r < R$, then H is on the same side of line $\overleftrightarrow{AI}$ as D.*

Proof. The proof of (1) is a basic construction: Construct the perpendicular bisector to DG. The point of intersection of that line with $\overleftrightarrow{FD}$ will be the center
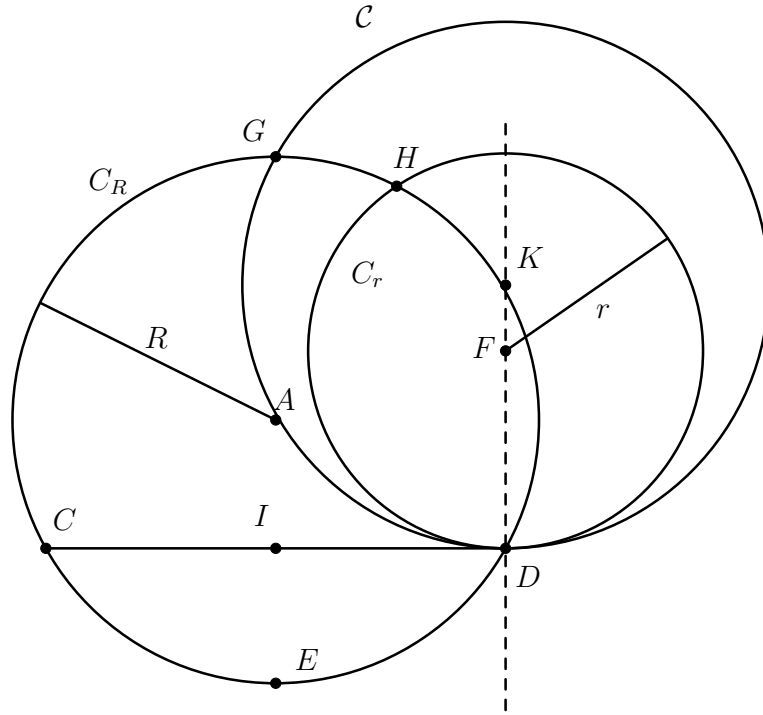
Figure A.6: A labeled picture of Lemma 3.

of $\mathcal{C}$. Call the center K. The radius calculation follows. This circle is clearly the unique circle tangent to CD at D which also goes through G.

To prove (2), let $a = |AI|$ and $b = |ID|$. Clearly $a^2 + b^2 = R^2$. Then the radius of $\mathcal{C}$ can be calculated as

$$|KD| = \frac{|IG|^2 + |ID|^2}{2|IG|} = \frac{(R+a)^2 + b^2}{2(R+a)} = \frac{2R(R+a)}{2(R+a)} = R.$$

This tells us that as $r \to R$, the point $H \to G$ and the circle $C_r \to \mathcal{C}$. This and a simple geometric argument proves that $G = H$ if and only if $r = R$. Lastly, any such circle C_r with radius $r < R$ tangent to CD at D will lie in the interior of $\mathcal{C}$ except for their single point of overlap, D. Then clearly by construction, H lies on the interior of arc $\overset{\frown}{DG}$, and hence is on the same side of line $\overleftrightarrow{AI}$ as point D. This completes the proof of Lemma 3. $\qquad\square$

We now have all of the pieces necessary to prove Proposition 12. Suppose that $\mu < \rho_{min}$ and consider a standard single particle trajectory, as seen in Figure A.7.
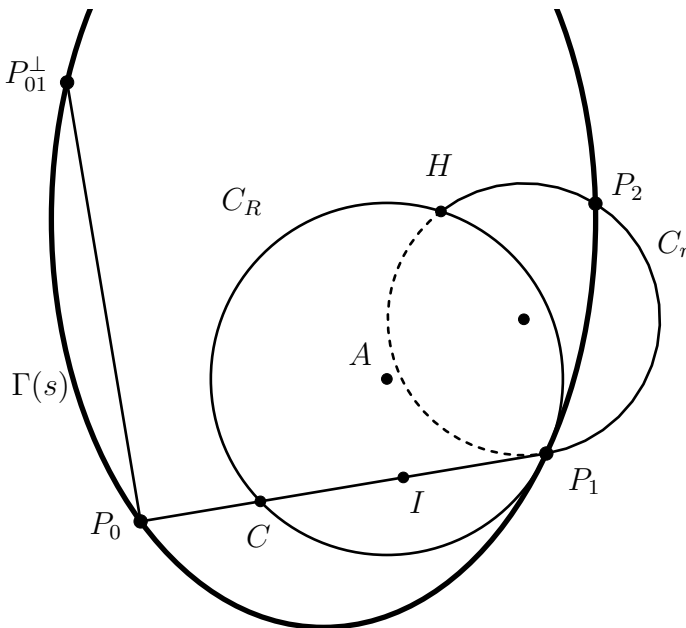
Figure A.7: A single trajectory arc, with labeling set as a mix of those from Lemma 3 and Figure A.4.

By Blaschke's Rolling Ball Theorem, we know that circle C_R with $R = 1/\kappa_{max} = \rho_{min}$ is contained entirely inside Ω. Furthermore, we know the circle C_r has radius $r = \mu$. By Lemma 3, we know that H and P_1 are on the same side of line $\overleftrightarrow{AI}$ as one another, and by construction are on the opposite side of $\overleftrightarrow{AI}$ from P_0 and $P_{01}^{\perp}$. And again by construction, the curve $\Gamma(s)$ first intersects C_r at P_1, but then must again intersect C_r at P_2. However now P_2 is on the interior of the counterclockwise arc from P_1 to H. This means the point P_2 lies on the same side of $\overleftrightarrow{AI}$ as P_1, and hence on the same side of $\overleftrightarrow{P_0 P_{01}^{\perp}}$ as P_1. Therefore the dot product

$$\overrightarrow{P_0 P_1} \cdot \overrightarrow{P_0 P_2} > 0$$

and therefore

$$\ell_1 + \ell_2 \cos(\chi) > 0.$$

This completes the proof of this geometric proposition.

A.5   Proof of Theorem 1

Following the proof from [BK96], we take our generating function

$$G(s_0, s_2) = -\ell_1 - |\gamma| + \frac{1}{\mu}\mathcal{S}$$

and break it into a magnetic field-dependent component and a magnetic field-independent component by writing $\mathcal{S} = Area(\mathcal{A} \cup \mathcal{S}) - \mathcal{A}$, where $\mathcal{A}$ is the area between the chord P_1, P_2 and the curve $\Gamma(s)$ (see Figure 2.1), and $Area(\mathcal{A} \cup \mathcal{S})$ is the area inside the circular arc γ cut by the chord $P_1 P_2$. This means we write

$$G(s_0, s_2) = \left[-\ell_1 - \frac{1}{\mu}\mathcal{A} \right] + \left[-|\gamma| + \frac{1}{\mu}Area(\mathcal{A} \cup \mathcal{S}) \right].$$

To proceed, we need information about $\mathcal{A}$, which we observe to be a function of s_1 and s_2.

Lemma 4. *Consider $\mathcal{A} = \mathcal{A}(s_1, s_2)$ defined as above. Then*

$$\frac{\partial \mathcal{A}}{\partial s_2} = \frac{1}{2}\ell_2 \sin(\chi - \theta_2).$$

Proof. Consider the chord $P_1 P_2$, and let $P_{2+h} := P_2 + h \cdot T_{P_2}\Gamma$, $h > 0$, be an approximation for $\Gamma(s_2 + h)$. Furthermore, let β be the angle between the vectors $\overrightarrow{P_2 P_1}$ and $\overrightarrow{P_2 P_{2+h}}$. Then the area of the triangle spanned by these two vectors is given by the magnitude of the cross product of these two vectors, which we easily

calculate as $\frac{1}{2}\ell_2 h \|T_{P_2}\Gamma\|\sin(\beta)$. However we see that $\beta = \pi - (\chi - \theta_2)$, and so

$$
\begin{aligned}
\frac{\partial \mathcal{A}}{\partial s_2} &= \lim_{h \to 0} \frac{\mathcal{A}(s_1, s_2 + h) - \mathcal{A}(s_1, s_2)}{h} \\
&= \lim_{h \to 0} \frac{\frac{1}{2}\ell_2 h \|T_{P_2}\Gamma\|\sin(\beta)}{h} \\
&= \lim_{h \to 0} \frac{1}{2}\ell_2 \sin(\pi - (\chi - \theta_2)) \\
&= \frac{1}{2}\ell_2 \sin(\chi - \theta_2).
\end{aligned}
$$

$\square$

Next, we recall a few useful formulas from earlier and from basic geometry:

$$
|\gamma| = \mu\psi = 2\mu\chi
$$

$$
Area(\mathcal{A} \cup \mathcal{S}) = \frac{\mu^2}{2}(\psi - \sin(\psi)) = \frac{\mu^2}{2}(2\chi - \sin(2\chi))
$$

$$
\frac{\partial \chi}{\partial s_2} = \frac{\cos(\chi - \theta_2)}{2\mu \cos(\chi)}
$$

$$
\sin(\chi) = \frac{\ell_2}{2\mu}.
$$

Thus

$$
\begin{aligned}
\frac{\partial G}{\partial s_2} &= 0 - \frac{1}{\mu}\frac{\partial \mathcal{A}}{\partial s_2} - \frac{\partial |\gamma|}{\partial \chi}\frac{\partial \chi}{\partial s_2} + \frac{1}{\mu}\frac{\partial Area(\mathcal{A} \cup \mathcal{S})}{\partial \chi}\frac{\partial \chi}{\partial s_2} \\
&= -\left(\frac{2}{\ell_2}\sin(\chi)\right)\left(\frac{\ell_2}{2}\sin(\chi - \theta_2)\right) - (2\mu)\left(\frac{\cos(\chi - \theta_2)}{2\mu \cos(\chi)}\right) \\
&\quad + \frac{\mu}{2}(2 - 2\cos(2\chi))\left(\frac{\cos(\chi - \theta_2)}{2\mu \cos(\chi)}\right) \\
&= -\sin(\chi)\sin(\chi - \theta_2) - \frac{\cos(\chi - \theta_2)}{\cos(\chi)} + \frac{\sin^2(\chi)\cos(\chi - \theta_2)}{\cos(\chi)} \\
&= -\sin(\chi)\sin(\chi - \theta_2) - \frac{\cos(\chi - \theta_2)}{\cos(\chi)}\left(1 - \sin^2(\chi)\right) \\
&= -\sin(\chi)\sin(\chi - \theta_2) - \cos(\chi)\cos(\chi - \theta_2)
\end{aligned}
$$

70

$$= -\cos(\chi - (\chi - \theta_2))$$

$$= -\cos(\theta_2)$$

$$= u_2.$$

And the calculation of the other partial derivative is simple since all factors of G except for ℓ_1 do not depend upon s_0. This is just repeating the calculation from the standard billiard map:

$$
\begin{aligned}
\frac{\partial G}{\partial s_0} &= -\frac{\partial \ell_1}{\partial s_0} \\
&= -\left.\frac{d}{dt}\right|_{t=s_0} \|\Gamma(t) - \Gamma(s_1)\| \\
&= -\left.\frac{d}{dt}\right|_{t=s_0} \langle \Gamma(t) - P_1, \Gamma(t) - P_1 \rangle^{1/2} \\
&= -\left.\frac{2\left\langle \dot{\Gamma}(t), \Gamma(t) - P_1 \right\rangle}{2\langle \Gamma(t) - P_1, \Gamma(t) - P_1 \rangle^{1/2}}\right|_{t=s_0} \\
&= \left.\frac{\left\langle \dot{\Gamma}(t), P_1 - \Gamma(t) \right\rangle}{\|\dot{\Gamma}(t)\|\|\Gamma(t) - P_1\|}\right|_{t=s_0} \\
&= \cos(\theta_0) \\
&= -u_0
\end{aligned}
$$

where $\langle \cdot, \cdot \rangle$ and $\| \cdot \|$ are the standard Euclidean inner product and norm, respectively. Together this means

$$
\begin{aligned}
dG &= \frac{\partial G}{\partial s_0} ds_0 + \frac{\partial G}{\partial s_2} ds_2 \\
&= -u_0 ds_0 + u_2 ds_2 \\
&= u_2 ds_2 - u_0 ds_0,
\end{aligned}
$$

and hence

$$G(s_0, s_2) = -\ell_1 - |\gamma| + \frac{1}{\mu}\mathcal{S}$$

is the generating function.

A.6 Proof of Proposition 9

Proof. We compute the coefficients in the Taylor expansion of our maps. This largely means evaluating each of our relevant partial derivatives at $\theta = 0$ and $\theta = \pi$. The first four are known ([Laz73]) while the others are new. Omitting the dependence on s,

$$\frac{\partial s_1}{\partial \theta_0}(s, 0) = \frac{2}{\kappa} = 2\rho$$

$$\frac{\partial^2 s_1}{\partial \theta_0^2}(s, 0) = -\frac{8}{3}\frac{\kappa'}{\kappa^3} = \frac{8}{3}\rho\rho'$$

$$\frac{\partial \theta_1}{\partial \theta_0}(s, 0) = 1$$

$$\frac{\partial^2 \theta_1}{\partial \theta_0^2}(s, 0) = \frac{4}{3}\frac{\kappa'}{\kappa^2} = -\frac{4}{3}\rho'$$

$$\frac{\partial s_2}{\partial \theta_1}(s, 0) = \frac{2\mu}{1 - \mu\kappa} = \frac{2\mu\rho}{\rho - \mu}$$

$$\frac{\partial^2 s_2}{\partial \theta_1^2}(s, 0) = \frac{4\mu^2\kappa'}{3(1 - \mu\kappa)^2} = -\frac{4\mu^2\rho'}{3(\rho - \mu)^2}$$

$$\frac{\partial \theta_2}{\partial \theta_1}(s, 0) = 1$$

$$\frac{\partial^2 \theta_2}{\partial \theta_1^2}(s, 0) = -\frac{2\mu\kappa'}{3(1 - \mu\kappa)} = \frac{2\mu\rho'}{3\rho(\rho - \mu)}$$

Similarly, remove the dependence on s and evaluate these derivatives at $\theta = \pi$. The first four are the same as above, while the others change:

$$\frac{\partial s_1}{\partial \theta_0}(s, \pi) = \frac{2}{\kappa} = 2\rho$$

$$\frac{\partial^2 s_1}{\partial \theta_0^2}(s, \pi) = -\frac{8}{3}\frac{\kappa'}{\kappa^3} = \frac{8}{3}\rho\rho'$$

$$\frac{\partial \theta_1}{\partial \theta_0}(s, \pi) = 1$$

$$\frac{\partial^2 \theta_1}{\partial \theta_0^2}(s, \pi) = \frac{4}{3}\frac{\kappa'(s)}{\kappa^2(s)} = -\frac{4}{3}\rho'$$

$$\frac{\partial s_2}{\partial \theta_1}(s, \pi) = -\frac{2\mu}{1 + \mu\kappa} = -\frac{2\mu\rho}{\rho + \mu}$$

$$\frac{\partial^2 s_2}{\partial \theta_1^2}(s, \pi) = \frac{4\mu^2\kappa'}{3(1 + \mu\kappa)^2} = -\frac{4\mu^2\rho'}{3(\rho + \mu)^2}$$

$$\frac{\partial \theta_2}{\partial \theta_1}(s, \pi) = 1$$

$$\frac{\partial^2 \theta_2}{\partial \theta_1^2}(s, \pi) = -\frac{2\mu\kappa'}{3(1 + \mu\kappa)} = \frac{\mu\rho'}{3\rho(\rho + \mu)}.$$

First we compute $\frac{\partial s_2}{\partial \theta_1}(s_1, \theta_1)$ near $\theta_1 = 0$. Using the approximations $\chi \approx \chi^*(\theta_1)$ from Proposition 1 and applying the l'Hopital rule in the second equality, we get

$$L := \lim_{\theta_1 \to 0^+} \frac{\ell_2 \cos(\chi)}{\sin(\theta_2)} = \lim_{\theta_1 \to 0^+} \frac{\frac{\partial \ell_2}{\partial s_2}\frac{\partial s_2}{\partial \theta_1}\cos(\chi) - \ell_2 \sin(\chi)\frac{\partial \chi}{\partial \theta_1}}{\cos(\theta_2)\frac{\partial \theta_2}{\partial \theta_1}}$$

$$= \lim_{\theta_1 \to 0^+} \frac{\cos(\chi - \theta_2)\frac{\partial s_2}{\partial \theta_1}\cos(\chi) - \ell_2 \sin(\chi)\frac{\partial \chi}{\partial \theta_1}}{\cos(\theta_2)\left[\frac{\sin(2\chi - \theta_2)}{\sin(\theta_2)} - \kappa_2 \frac{\ell_2 \cos(\chi)}{\sin(\theta_2)}\right]} = \lim_{\theta_1 \to 0^+} \frac{\frac{\ell_2 \cos(\chi)}{\sin(\theta_1)} + O(\theta_1^2)}{2c - 1 - \kappa \frac{\ell_2 \cos(\chi)}{\sin(\theta_1)} + O(\theta_1^2)},$$

where the last line is the Taylor expansions of the numerator and denominator near 0 and noting that $\theta_2 \approx \theta_1$ when θ_1 is small and letting $c = \frac{\rho_1}{\rho_1 - \mu} = \frac{1}{1 - \mu\kappa_1}$. This tells us that

$$L = \frac{L}{2c - 1 - \kappa_1 L}.$$

It follows from the convexity of $\Gamma(s)$ and [KS86] (Theorem 4.3 in Part V) that $L < \infty$, so $L = 0$ or $L = \frac{2c - 2}{\kappa_1}$. We wish to show that $L > 0$. Consider the osculating circle $\mathcal{O}_\Gamma(s_2)$ at $\Gamma(s_2)$ with radius ρ_2. Then via elementary geometry, the length of the chord ℓ_2 that is inside $\mathcal{O}_\Gamma(s_2)$ is exactly $2\rho_2 \sin(\theta_2)$. Therefore

$\ell_2 \geq 2\rho_2 \sin(\theta_2)$, and so

$$L \geq 2\cos(\chi)\rho_{min} > 0.$$

This means $L = \frac{\partial s_2}{\partial \theta_1}(s, 0) = \frac{2c-2}{\kappa_1} = \frac{2\mu}{1-\mu\kappa_1}$.

Next, we see that

$$\frac{\partial \theta_2}{\partial \theta_1}(s_1, 0) := \lim_{\theta_1 \to 0^+} \frac{\partial \theta_2}{\partial \theta_1}(s, \theta_1) = \lim_{\theta_1 \to 0^+} \frac{\sin(2\chi - \theta_2)}{\sin(\theta_2)} - \kappa_2 \frac{\partial s_2}{\partial \theta_1}$$

$$= \lim_{\theta_1 \to 0^+} (2c-1) + O(\theta_1^2) - \kappa\left(\frac{2c-2}{\kappa}\right) = 2c - 1 - (2c-2) = 1.$$

To compute the second order terms, we will need two expansions of terms we have seen prior. The Taylor expansions of ℓ_2 and $\frac{\partial \theta_2}{\partial \theta_1}$ around $\theta_1 = 0$ are

$$\ell_2(s_1, s_2) \approx \ell_2(s_1, s_1) + \frac{\partial \ell_2}{\partial s_2}\frac{\partial s_2}{\partial \theta_1}\theta_1 + O(\theta_1^2) = \cos(\chi - \theta_2)\frac{\partial s_2}{\partial \theta_1}(s_1, 0)\theta_1 + O(\theta_1^2)$$

$$\frac{\partial \theta_2}{\partial \theta_1}(s_1, \theta_1) \approx \frac{\partial \theta_2}{\partial \theta_1}(s_1, 0) + \frac{\partial^2 \theta_2}{\partial \theta_1^2}(s_1, 0)\theta_1 + O(\theta_1^2) = 1 + \frac{\partial^2 \theta_2}{\partial \theta_1^2}(s_1, 0)\theta_1 + O(\theta_1^2).$$

Observe that

$$\frac{\partial^2 s_2}{\partial \theta_1^2}(s_1, 0) := \lim_{\theta_1 \to 0^+} \frac{\partial^2 s_2}{\partial \theta_1^2} = \lim_{\theta_1 \to 0^+} \frac{\partial}{\partial \theta_1}\left(\frac{\ell_2 \cos(\chi)}{\sin(\theta_2)}\right)$$

$$= \lim_{\theta_1 \to 0^+} \frac{\sin(\theta_2)(\frac{\partial \ell_2}{\partial s_2}\frac{\partial s_2}{\partial \theta_1}\cos(\chi) - \ell_2 \sin(\chi)\frac{\partial \chi}{\partial \theta_1}) - \ell_2 \cos(\chi)\cos(\theta_2)\frac{\partial \theta_2}{\partial \theta_1}}{\sin^2(\theta_2)}$$

$$= \lim_{\theta_1 \to 0^+} \frac{\cos(\chi - \theta_2)\frac{\partial s_2}{\partial \theta_1}\cos(\chi) - (\cos(\chi - \theta_2)\frac{\partial s_2}{\partial \theta_1}(s_1, 0)\theta_1 + O(\theta_1^2))\sin(\chi)\frac{\partial \chi}{\partial \theta_1}}{\sin(\theta_2)}$$

$$- \frac{(\cos(\chi - \theta_2)\frac{\partial s_2}{\partial \theta_1}(s_1, 0)\theta_1 + O(\theta_1^2))\cos(\chi)\cot(\theta_2)(1 + \frac{\partial^2 \theta_2}{\partial \theta_1^2}(s_1, 0)\theta_1 + O(\theta_1^2))}{\sin(\theta_2)}$$

$$= \lim_{\theta_1 \to 0^+} \frac{\frac{\partial s_2}{\partial \theta_1}\cos(\chi - \theta_2)(\cos(\chi) - \theta_1 \sin(\chi)\frac{\partial \chi}{\partial \theta_1}}{\sin(\theta_2)}$$

$$- \frac{\theta_1 \cos(\chi)\cot(\theta_2)(1 + \frac{\partial^2 \theta_2}{\partial \theta_1^2}(s_1, 0)\theta_1 + O(\theta_1^2)))}{\sin(\theta_2)}$$

$$= -\frac{\partial s_2}{\partial \theta_1}(s_1, 0)\frac{\partial^2 \theta_2}{\partial \theta_1^2}(s_1, 0) = -\left(\frac{2c-2}{\kappa}\right)\frac{\partial^2 \theta_2}{\partial \theta_1^2}(s_1, 0)$$

74

and

$$\frac{\partial^2 \theta_2}{\partial \theta_1^2}(s_1, 0) := \lim_{\theta_1 \to 0^+} \frac{\partial^2 \theta_2}{\partial \theta_1^2} = \lim_{\theta_1 \to 0^+} \frac{\partial}{\partial \theta_1}\left(\frac{\sin(2\chi - \theta_2)}{\sin(\theta_2)} - \kappa_2 \frac{\partial s_2}{\partial \theta_1}\right)$$

$$= \lim_{\theta_1 \to 0^+} \frac{\cos(2\chi - \theta_2)(2\frac{\partial \chi}{\partial \theta_1} - \frac{\partial \theta_2}{\partial \theta_1}) - \sin(2\chi - \theta_2)\cot(\theta_2)\frac{\partial \theta_2}{\partial \theta_1}}{\sin^2(\theta_2)} - \left(\kappa_2 \frac{\partial^2 s_2}{\partial \theta_1^2} + \kappa_2' \frac{\partial s_2}{\partial \theta_1}\right)$$

$$= \lim_{\theta_1 \to 0^+} -\left(\kappa_2 \frac{\partial^2 s_2}{\partial \theta_1^2} + \left(\frac{\partial s_2}{\partial \theta_1}(s_1, 0) + \frac{\partial^2 s_2}{\partial \theta_1^2}\theta_1 + O(\theta_1^2)\right)\kappa'(s_2)\right)$$

$$+ \frac{\cos(2\chi - \theta_2)(2\frac{\partial \chi}{\partial \theta_1} - (1 + \frac{\partial^2 \theta_2}{\partial \theta_1^2}(s_1, 0)\theta_1 + O(\theta_1^2)))}{\sin(\theta_2)}$$

$$- \frac{\sin(2\chi - \theta_2)\cot(\theta_2)(1 + \frac{\partial^2 \theta_2}{\partial \theta_1^2}(s_1, 0) + O(\theta_1^2))}{\sin(\theta_2)}$$

$$= -2c\frac{\partial^2 \theta_2}{\partial \theta_1^2}(s_1, 0) - \frac{\partial^2 s_2}{\partial \theta_1^2}(s_1, 0) - \left(\frac{2c - 2}{\kappa}\right)\kappa'.$$

We then solve the system

$$\frac{\partial^2 s_2}{\partial \theta_1^2}(s_1, 0) = -\left(\frac{2c - 2}{\kappa}\right)\frac{\partial^2 \theta_2}{\partial \theta_1^2}(s_1, 0)$$

$$\frac{\partial^2 \theta_2}{\partial \theta_1^2}(s_1, 0) = -2c\frac{\partial^2 \theta_2}{\partial \theta_1^2}(s_1, 0) - \frac{\partial^2 s_2}{\partial \theta_1^2}(s_1, 0) - \left(\frac{2c - 2}{\kappa}\right)\kappa'$$

to get that

$$\frac{\partial^2 s_2}{\partial \theta_1^2}(s_1, 0) = \frac{(2c - 2)^2 \kappa'}{3\kappa^2} = \frac{4\mu^2 \kappa'}{3(1 - \mu\kappa)^2}$$

$$\frac{\partial^2 \theta_2}{\partial \theta_1^2}(s_1, 0) = -\frac{(2c - 2)\kappa'}{3\kappa} = -\frac{2\mu\kappa'}{3(1 - \mu\kappa)}.$$

Repeating these calculations for the other approximation of $\chi \approx \chi^*$ yields the same result. Near $\theta_1 = \pi - \eta_1$, performing the same calculations above we get the results in the summary above. To get the results stated in the theorem, we also

75

then use the Taylor expansions in θ_1

$$s_2 = s_1 + \frac{\partial s_2}{\partial \theta_1}(s_1, 0)\theta_1 + \frac{1}{2}\frac{\partial^2 s_2}{\partial \theta_1^2}(s_1, 0)\theta_1^2 + O(\theta_1^3)$$

$$\theta_2 = \frac{\partial \theta_2}{\partial \theta_1}(s_1, 0)\theta_1 + \frac{1}{2}\frac{\partial^2 \theta_2}{\partial \theta_1^2}(s_1, 0)\theta_1^2 + O(\theta_1^3)$$

and writing $\theta_i = \pi - \eta_i$,

$$s_2 = s_1 - \frac{\partial s_2}{\partial \theta_1}(s_1, \pi)\eta_1 + \frac{1}{2}\frac{\partial^2 s_2}{\partial \theta_1^2}(s_1, \pi)\eta_1^2 + O(\eta_1^3)$$

$$\eta_2 = \frac{\partial \theta_2}{\partial \theta_1}(s_1, \pi)\theta_1 - \frac{1}{2}\frac{\partial^2 \theta_2}{\partial \theta_1^2}(s_1, \pi)\eta_1^2 + O(\eta_1^3).$$

$\square$

Bibliography

[Ami97]   Edoh Amiran, *Integrable smooth planar billiards and evolutes*, New York Journal of Mathematics **3** (1997), 32–47.

[Ber96]   N Berglund, *Billiards in a potential: variational methods, periodic orbits, and KAM tori*, Preprint, 1996.

[Bir27]   G.D. Birkhoff, *Dynamical Systems*, American Mathematical Society / Providence, RI, American Mathematical Society, 1927.

[BK96]   N. Berglund and H. Kunz, *Integrability and ergodicity of classical billiards in a magnetic field*, Journal of Statistical Physics **83** (1996), no. 1-2, 81–126.

[Bla16]   W. Blaschke, *Kreis und Kugel*, zweite ed., Veit, 1916.

[CM06]   Nikolai Chernov and Roberto Markarian, *Chaotic Billiards*, American Mathematical Soc., 2006.

[CP12]   Giulio Casati and Tomaž Prosen, *Time Irreversible Billiards with Piecewise-Straight Trajectories*, Phys. Rev. Lett. **109** (2012), no. 17, 174101.

[Dou82]   Raphael Douady, *Applications du théoréme des tores invariants*, Ph.D. thesis, Université Paris VII, 1982.

[dSKW17] Jacopo de Simoi, Vadim Kaloshin, and Qiaoling Wei, *Dynamical spectral rigidity among $\mathbb{Z}_2$-symmetric strictly convex domains close to a circle*, Annals of Mathematics **186** (2017), no. 1, 277–314.

[Gol01]   C. Golé, *Symplectic Twist Maps: Global Variational Techniques*, Advanced series in nonlinear dynamics, World Scientific, 2001.

[Hub87]   Andrea Hubacher, *Instability of the boundary in the billiard ball problem*, Commun.Math. Phys. **108** (1987), no. 3, 483–488.

[KPC05]   Bence Kocsis, Gergely Palla, and József Cserti, *Quantum and semi-classical study of magnetic quantum dots*, Physical Review B **71** (2005), no. 7, 075331.

[KROC08]   A. Kormányos, P. Rakyta, L. Oroszlány, and J. Cserti, *Bound states in inhomogeneous magnetic field in graphene: Semiclassical approach*, Phys. Rev. B **78** (2008), no. 4, 045430.

[KS86]   Anatole Katok and Jean-Marie Strelcyn, *Invariant manifolds, entropy and billiards: smooth maps with singularities*, Lecture notes in mathematics, no. 1222, Springer, Berlin, 1986, OCLC: 15018884.

[KS17]   Andreas Knauf and Marcello Seri, *Symbolic dynamics of magnetic bumps*, Regul. Chaot. Dyn. **22** (2017), no. 4, 448–454.

[KSS13]   Andreas Knauf, Frank Schulz, and Karl Friedrich Siburg, *Positive topological entropy for multi-bump magnetic fields*, Nonlinearity **26** (2013), no. 3, 727–743.

[KT91]   V.V. Kozlov and D.V. Treshchëv, *Billiards: A Genetic Introduction to the Dynamics of Systems with Impacts: A Genetic Introduction to the Dynamics of Systems with Impacts*, Translations of Mathematical Monographs, American Mathematical Society, 1991.

[KZ18]   Vadim Kaloshin and Ke Zhang, *Density of convex billiards with rational caustics*, Nonlinearity **31** (2018), no. 11, 5214–5234.

[Laz73]   V F Lazutkin, *The Existence of Caustics for a Billiard Problem in a Convex Domain*, Mathematics of the USSR-Izvestiya **7** (1973), no. 1, 185–214.

[Mat82]   John N. Mather, *Glancing billiards*, Ergodic Theory and Dynamical Systems **2** (1982), no. 3-4, 397–403.

[MBG93]   O Meplan, F Brut, and C Gignoux, *Tangent map for classical billiards in magnetic fields*, J. Phys. A: Math. Gen. **26** (1993), no. 2, 237–246.

[Mei92]   J. D. Meiss, *Symplectic maps, variational principles, and transport*, Reviews of Modern Physics **64** (1992), no. 3, 795–848.

[MF94]   John N. Mather and Giovanni Forni, *Action minimizing orbits in hamiltomian systems*, Transition to Chaos in Classical and Quantum Mechanics: Lectures given at the 3rd Session of the Centro Internazionale Matematico Estivo (C.I.M.E.) held in Montecatini Terme, Italy, July 6-13, 1991 (Sandro Graffi, ed.), Springer Berlin Heidelberg, Berlin, Heidelberg, 1994, pp. 92–186.

[Mos62]   J. Moser, *On Invariant Curves of Area-preserving Mappings of an Annulus*, Nachrichten der Akademie der Wissenschaften in Göttingen: II, Mathematisch-Physikalische Klasse, Vandenhoeck & Ruprecht, 1962.

[Mos16]   _____, *Stable and Random Motions in Dynamical Systems: With Special Emphasis on Celestial Mechanics (AM-77)*, Princeton Landmarks in Mathematics and Physics, Princeton University Press, 2016.

[MRRTS16] Pau Martín, Rafael Ramírez-Ros, and Anna Tamarit-Sariol, *On the length and area spectrum of analytic convex domains*, Nonlinearity **29** (2016), no. 1, 198–231.

[Nog10]   Alain Nogaret, *Electron dynamics in inhomogeneous magnetic fields*, Journal of Physics: Condensed Matter **22** (2010), no. 25, 253201.

[RB85]   M Robnik and M V Berry, *Classical billiards in magnetic fields*, J. Phys. A: Math. Gen. **18** (1985), no. 9, 1361–1378.

[Rob86]   Marko Robnik, *Regular and chaotic billiard dynamics in magnetic fields*, Nonlinear Phenomena and Chaos **1** (1986), 303–330.

[SG10]   Yu Song and Yong Guo, *Bound states in a hybrid magnetic-electric quantum dot*, Journal of Applied Physics **108** (2010), no. 6, 064306.

[SIKL98]   Heung-Sun Sim, G Ihm, N Kim, and S J Lee, *Magnetic Edge States in a Magnetic Quantum Dot*, Physical Review Letters **80** (1998), no. 7, 4.

[SLA12]   J. Szücs, M. Levi, and V.I. Arnol'd, *Geometrical Methods in the Theory of Ordinary Differential Equations*, Grundlehren der mathematischen Wissenschaften, Springer New York, 2012.

[Sor18]   A Sorrentino, *Some Computations*, Unpublished notes, 2018.

[Tas97]   Tamás Tasnádi, *Hard Chaos in Magnetic Billiards (On the Euclidean Plane)*, Communications in Mathematical Physics **187** (1997), no. 3, 597–621.

[TS05]   S. Tabachnikov and Pennsylvania State University Mathematics Advanced Study Semesters, *Geometry and Billiards*, Student mathematical library, American Mathematical Society, 2005.

[VTCP03]   Z. Vörös, T. Tasnádi, J. Cserti, and P. Pollner, *Tunable Lyapunov exponent in inverse magnetic billiards*, Physical Review E **67** (2003), no. 6, 065202.

[VWA97]   K. Vogtmann, A. Weinstein, and V.I. Arnol'd, *Mathematical Methods of Classical Mechanics*, Graduate Texts in Mathematics, Springer New York, 1997.